AMERICAN SOCIETY FOR MICROBIOLOGY | Journal of Virology®

Human Asymptomatic Epitopes Identified from the Herpes Simplex Virus Tegument Protein VP13/14 (UL47) Preferentially Recall Polyfunctional Effector Memory CD44^{high} CD62L^{low} CD8$^+$ T_{EM} Cells and Protect Humanized HLA-A*02:01 Transgenic Mice against Ocular Herpesvirus Infection

Ruchi Srivastava,[a] Arif A. Khan,[a] Sumit Garg,[a] Sabrina A. Syed,[a] Julie N. Furness,[a] Hawa Vahed,[a] Tiffany Pham,[a] Howard T. Yu,[a] Anthony B. Nesburn,[a] Lbachir BenMohamed[a,b,c]

Laboratory of Cellular and Molecular Immunology, Gavin Herbert Eye Institute, University of California, Irvine, School of Medicine, Irvine, California, USA[a]; Department of Molecular Biology & Biochemistry[b] and Institute for Immunology,[c] University of California, Irvine, School of Medicine, Irvine, California, USA

ABSTRACT Herpes simplex virus 1 (HSV-1) infection is widespread among humans. The HSV-1 virion protein 13/14 (VP13/14), also known as UL47, is a tegument antigen targeted by CD8$^+$ T cells from HSV-seropositive individuals. However, whether VP13/14-specific CD8$^+$ T cells play a role in the natural protection seen in asymptomatic (ASYMP) individuals (individuals who have never had a clinical herpetic disease) has not been elucidated. Using predictive computer-assisted algorithms, we identified 10 potential HLA-A*02:01-restricted CD8$^+$ T-cell epitopes from the 693-amino-acid sequence of the VP13/14 protein. Three out of 10 epitopes exhibited a high to moderate affinity of binding to soluble HLA-A*02:01 molecules. The phenotype and function of CD8$^+$ T cells specific for each epitope were compared in HLA-A*02:01-positive ASYMP individuals and symptomatic (SYMP) individuals (individuals who have frequent clinical herpetic diseases) using determination of a combination of tetramer frequency and the levels of granzyme B, granzyme K, perforin, gamma interferon, tumor necrosis factor alpha, and interleukin-2 production and CD107$^{a/b}$ cytotoxic degranulation. High frequencies of multifunctional CD8$^+$ T cells directed against three epitopes, VP13/14 from amino acids 286 to 294 (VP13/14$_{286-294}$), VP13/14 from amino acids 504 to 512 (VP13/14$_{504-512}$), and VP13/14 from amino acids 544 to 552 (VP13/14$_{544-552}$), were detected in ASYMP individuals, while only low frequencies were detected in SYMP individuals. The three epitopes also predominantly recalled more CD45RA^{low} CD44^{high} CCR7^{low} CD62L^{low} CD8$^+$ effector memory T cells (T_{EM} cells) in ASYMP individuals than SYMP individuals. Moreover, immunization of HLA-A*02:01 transgenic mice with the three CD8$^+$ T_{EM}-cell epitopes from ASYMP individuals induced robust and polyfunctional HSV-specific CD8$^+$ T_{EM} cells associated with strong protective immunity against ocular herpesvirus infection and disease. Our findings outline the phenotypic and functional features of protective HSV-specific CD8$^+$ T cells that should guide the development of a safe and effective T-cell-based herpes simplex vaccine.

IMPORTANCE Although most herpes simplex virus 1 (HSV-1)-infected individuals shed the virus in their body fluids following reactivation from latently infected sen-

Received 6 September 2016 **Accepted** 29 September 2016

Accepted manuscript posted online 9 November 2016

Citation Srivastava R, Khan AA, Garg S, Syed SA, Furness JN, Vahed H, Pham T, Yu HT, Nesburn AB, BenMohamed L. 2017. Human asymptomatic epitopes identified from the herpes simplex virus tegument protein VP13/14 (UL47) preferentially recall polyfunctional effector memory CD44^{high} CD62L^{low} CD8$^+$ T_{EM} cells and protect humanized HLA-A*02:01 transgenic mice against ocular herpesvirus infection. J Virol 91:e01793-16. https://doi.org/10.1128/JVI.01793-16.

Editor Jae U. Jung, University of Southern California

Address correspondence to Lbachir BenMohamed, Lbenmoha@uci.edu.

This paper is dedicated to our longtime collaborator and colleague Steven L. Wechsler, who passed away unexpectedly on 12 June 2016.

sory ganglia, the majority never develop a recurrent herpetic disease and remain asymptomatic (ASYMP). In contrast, small proportions of individuals are symptomatic (SYMP) and develop frequent bouts of recurrent disease. The present study demonstrates that naturally protected ASYMP individuals have a higher frequency of effector memory CD8$^+$ T cells (CD8$^+$ T_{EM} cells) specific to three epitopes derived from the HSV-1 tegument protein VP13/14 (VP13/14$_{286-294}$, VP13/14$_{504-512}$, and VP13/14$_{544-552}$) than SYMP patients. Moreover, immunization of humanized HLA-A*02:01 transgenic mice with the three CD8$^+$ T_{EM}-cell epitopes from ASYMP individuals induced robust and polyfunctional HSV-specific CD8$^+$ T cells associated with strong protective immunity against ocular herpesvirus infection and disease. The findings support the emerging concept of the development of a safe and effective asymptomatic herpes simplex vaccine that is selectively based on CD8$^+$ T-cell epitopes from ASYMP individuals.

KEYWORDS granzyme B, granzyme K, HSV, herpes simplex virus, human leukocyte antigen, memory CD8$^+$ T cells, perforin, transgenic, virion phosphoprotein, humans, immunization

A staggering 3.72 billion individuals worldwide (i.e., over 52% of the world's population) are currently infected with herpes simplex virus 1 (HSV-1), which causes a wide range of recurrent diseases throughout their lives (1–3). After primary (1°) ocular HSV-1 infection, the virus establishes latency in the sensory neurons of human trigeminal ganglia (TG), a state that lasts for the life of the host (1, 4–6). Sporadic reactivation of the virus from latently infected sensory neurons of TG produces virus shedding in tears, which can lead to either relatively harmless asymptomatic (ASYMP) secondary (2°) reinfection of the cornea (COR) or symptomatic (SYMP) recurrent corneal disease and potentially blinding herpetic stromal keratitis (HSK) (5–8). The majority of HSV-seropositive individuals are ASYMP (9–12). They do not experience any recurrent herpetic disease, even though the virus spontaneously reactivates from latency and sheds multiple times each year in their tears (13–16). In contrast, a small proportion of HSV-seropositive individuals are SYMP and experience lifelong recurrences of herpetic disease, usually multiple times a year (17, 18), and often require continuous antiviral therapy (i.e., acyclovir and derivatives).

In HSV-seropositive SYMP individuals, sporadic reactivation of the virus from latency and its shedding in tears can cause blinding recurrent herpetic stromal keratitis (rHSK), a T-cell-mediated immunopathological lesion of the cornea (2, 19, 20). Vaccine clinical trials throughout the last 2 decades have concentrated on the antibody responses induced by HSV envelope glycoproteins gB and gD, which have failed to produce protective immunity (21, 22). Thus, it is necessary to identify and evaluate more protective T-cell-based HSV antigens (Ags).

Among the 84-plus open reading frames (ORFs) of the HSV-1 genome, those encoding tegument protein Ags are the least immunologically characterized (9–12). In animal models of herpesvirus infection and disease, HSV-specific CD8$^+$ T cells play a critical role in aborting attempts of virus reactivation from latency and in clearing herpetic disease (2, 4, 14, 23–25). However, herpetic corneal disease is also associated with HSV-specific CD8$^+$ T-cell responses (26, 27). Identification of CD8$^+$ T-cell epitopes from tegument proteins will aid herpes simplex vaccine design by the incorporation of protective epitopes from the HSV-1 VP13/14 tegument protein from ASYMP individuals (referred to here as ASYMP epitopes) into vaccines and allow detailed phenotypic and functional characterization of the protective CD8$^+$ T cells. A previous report showed that some epitopes from the virion protein 13/14 (VP13/14) tegument protein are recognized by human CD8$^+$ T cells from HSV-seropositive individuals in the context of human leukocyte antigen (HLA)-A*02:01 (28). However, the repertoire of HSV-1 VP13/14 epitopes that are exclusively recognized by CD8$^+$ T cells from naturally protected ASYMP individuals and the phenotype and function of VP13/14 epitope-specific CD8$^+$ T cells involved in protective immunity have never been reported.

TABLE 1 Potential HLA-A*02:01-restricted epitopes selected from HSV VP13/14[a]

Epitope	Sequence	Mol wt	No. of amino acids	IC_{50} (nM)				
				BIMAS	SYFPEITHI	MAPPP	MHCPred	HLA-A*201
$VP13/14_{286–294}$	**FLADAVVRL**	1003.2	9	926.658	30	ND	0.41	5.6
$VP13/14_{374–382}$	ALLDRDCRV	1060.2	9	1055.1	25	0.7512	0.27	52
$VP13/14_{410–418}$	VLTREAAFL	1019.2	9	199.738	22	ND	0.43	
$VP13/14_{417–425}$	FLGRVLDVL	1131.2	9	45.406	25	ND	0.38	
$VP13/14_{464–472}$	ALPLGSPAV	823.9	9	69.552	26	0.5393	0.26	
$VP13/14_{497–505}$	VLGAAVYAL	876.0	9	83.527	27	0.5307	0.45	100
$VP13/14_{504–512}$	**ALHTALATV**	896.0	9	159.97	30	0.6459	0.20	16
$VP13/14_{544–552}$	**RLLGFADTV**	991.1	9	479.172	27	0.6928	0.24	27
$VP13/14_{545–553}$	LLGFADTVV	934.1	9	48.478	21	ND	0.18	
$VP13/14_{657–665}$	IMSQFRKLL	1,135.4	9	99.667	20	0.9931	0.42	

[a]The sequence of the HSV-1 tegument protein VP13/14 was submitted to screening for potential HLA-A*0201 epitopes using several computer algorithms. The 10 potential epitopes were selected on the basis of the HLA-A*0201-binding amino acid motifs. The predicted IC_{50}s were calculated by use of the (i) BIMAS (http://www-bimas.cit.nih.gov/molbio/hla_bind) (ii) SYFPEITHI (http://www.syfpeithi.de/), (iii) MAPPP (http://www.mpiib-berlin.mpg.de/MAPPP), and (iv) MHCPred predictive computational algorithms, as described in Materials and Methods. The sequences of the peptide epitopes are based on the sequences of VP13/14 from HSV-1 strain 17. Sequences in bold are immunodominant epitopes from asymptomatic individuals. ND, not determined.

In the present study, we sought to identify the protective ASYMP epitopes from the HSV-1 VP13/14 tegument protein. We report three novel protective epitopes that were strongly recognized by $CD8^+$ T cells from HSV-seropositive healthy ASYMP individuals (VP13/14 from amino acids 286 to 294 [$VP13/14_{286–294}$], VP13/14 from amino acids 504 to 512 [$VP13/14_{504–512}$], and VP13/14 from amino acids 544 to 552 [$VP13/14_{544–552}$]). Frequent, robust, and polyfunctional effector $CD8^+$ T-cell responses were predominantly directed against these three epitopes in ASYMP individuals but not in SYMP patients. A significantly higher proportion of effector memory $CD8^+$ T cells (T_{EM} cells) recognizing these three HSV-1 VP13/14 epitopes were detected in naturally protected ASYMP individuals than in SYMP patients. Moreover, immunization of HLA transgenic (Tg) mice with the three VP13/14 $CD8^+$ T-cell epitopes induced strong protective immunity against ocular herpesvirus infection and disease. Altogether, our findings identify previously unknown protective epitopes from the VP13/14 tegument protein and delineate quantitative and qualitative features of protective HSV-specific $CD8^+$ T cells that should be taken into consideration for the development of a T-cell-based herpes simplex vaccine.

RESULTS

***In silico* prediction of potential HLA-A*02:01-restricted T-cell epitopes from the HSV-1 VP13/14 protein.** The amino acid sequence of the HSV-1 VP13/14 tegument protein (strain 17) was screened for potential HLA-A*02:01-binding regions using the BIMAS, SYFPEITHI, and MAPPP predictive computational algorithms (4). On the basis of the results of these analyses, we identified 10 potential epitopes with a high predicted affinity to HLA-A*02:01 molecules (Table 1). We chose the HLA-A*02:01 haplotype because it is prevalent in over 50% of the world's population, regardless of gender and ethnicity (29). All 10 VP13/14 epitopes shared the HLA-A*02:01-binding motifs: leucine or valine at the second position and a leucine, valine, methionine, or alanine at the ninth position. On the basis of the computational algorithms listed above, these VP13/14 epitopes bear putative antigenic and immunogenic HLA-A*02:01-binding regions and thus are more likely to be less constrained than other parts of the VP13/14 molecule, resulting in increased accessibility to proteolysis, an event that precedes T-cell epitope presentation in association with an HLA molecule (30–35).

Three out of 10 potential VP13/14 epitopes bind and stabilize HLA-A*02:01 molecules on the surface of target cells. Peptides corresponding to the 10 highly probable VP13/14 epitopes were synthesized and experimentally tested for their affinity of binding to soluble HLA-A*02:01 molecules (Table 1). The $VP13/14_{286–294}$ peptide showed the highest affinity of binding to soluble HLA-A*02:01 molecules (equilibrium dissociation constant [K_D], 5.6 nM). Peptides $VP13/14_{504–512}$ and $VP13/14_{544–552}$ showed a medium affinity of binding to soluble HLA-A*02:01 molecules (K_Ds,

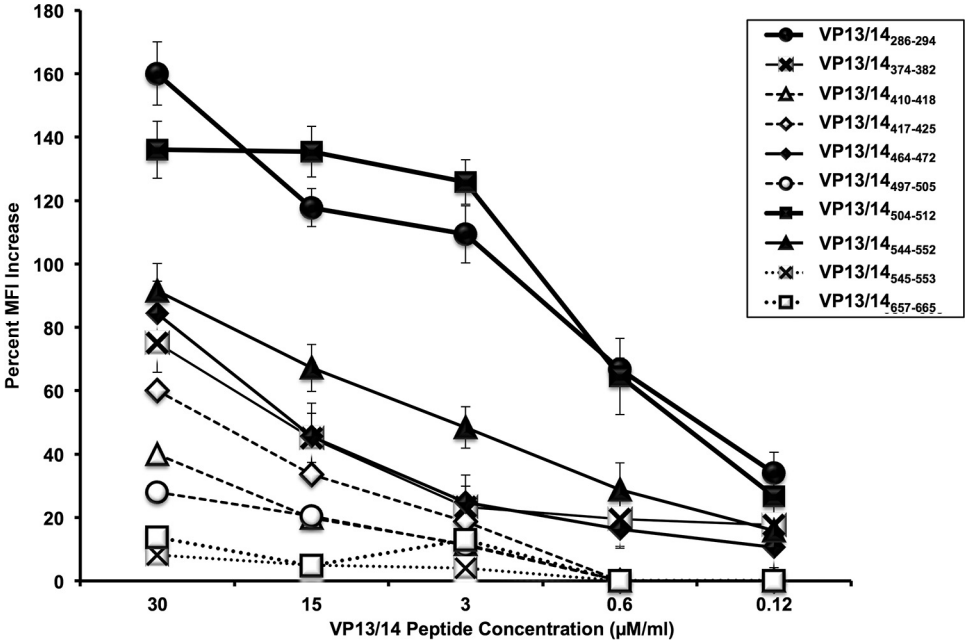

FIG 1 Stabilization of HLA-A*02:01 molecules on the surface of T2 cells by VP13/14 peptide epitopes. T2 cells (3×10^5) were incubated with serial dilutions of the indicated VP13/14 peptide, as described in Materials and Methods. Cells were then stained with an FITC-conjugated anti-HLA-A2 MAb (BB7.2). The graph represents the increase in the expression of HLA-A2 molecules on the surface of T2 cells triggered by various concentrations of VP13/14 peptides, and the data represent the percent MFI increase, which was calculated as follows: [(MFI with the given peptide − MFI without peptide)/(MFI without peptide)] × 100. Solid lines, peptides that bind to HLA-A02:01 molecules with a moderate to high affinity; broken lines, peptides that bind to HLA-A02:01 molecules with a low affinity. Error bars show SDs obtained from 3 independent experiments.

16 nM and 27 nM, respectively). The remaining seven peptides showed no significant affinity of binding to HLA-A*02:01 molecules.

Cell surface expression of HLA-A*02:01 molecules depends primarily on peptide transport into the endoplasmic reticulum/Golgi apparatus by the transporter associated with antigen processing (TAP). Cells of class I HLA-transfected B × T hybrid cell lines (T2 lines) are deficient in TAP but still express small amounts of major histocompatibility complex (MHC) class I on their surface (4). We next performed an assay for the stabilization of HLA-A*02:01 molecules on T2 cells. The T2 cell-binding assay is based on the ability of peptides to stabilize the MHC class I complex on the surface of cells of the T2 cell line. Each of the 10 VP13/14 peptides was tested at escalating doses of 0.1 μM, 0.6 μM, 3 μM, 15 μM, and 30 μM (Fig. 1). Out of 10 VP13/14 peptides, the VP13/$14_{286-294}$ andVP13/$14_{504-512}$ peptides showed the highest affinity of binding to HLA-A*02:01 molecules. These two peptides significantly increased the levels of HLA-A*02:01 molecules on the surface of the T2 cells in a dose-dependent manner ($P < 0.001$). Of the remaining eight peptides, VP13/$14_{544-552}$ had a medium affinity of binding to HLA-A*02:01 molecules (Fig. 1) Despite many attempts, the remaining seven peptides produced no significant stabilization of HLA-A*02:01 molecules on the surface of T2 cells (Fig. 1).

The aforementioned results suggest that 3 out of 10 potential VP13/14 peptides, VP13/$14_{286-294}$,VP13/$14_{504-512}$, and VP13/$14_{544-552}$, bind with a high to moderate affinity to HLA-A*02:01 molecules and significantly increase the levels of HLA-A*02:01 molecules on the surface of target cells. Therefore, these three peptides might lead to the efficient functional presentation of HLA-A*02:01 molecules and the stimulation of $CD8^+$ T cells.

High frequency of detection of VP13/$14_{286-294}$-, VP13/$14_{504-512}$-, and VP13/$14_{544-552}$-specific $CD8^+$ T cells in HLA-A*02:01-positive, HSV-seropositive ASYMP individuals. We segregated 20 HLA-A*02:01-positive, HSV-1-seropositive individuals into two groups: (i) 10 asymptomatic (ASYMP) individuals who had never had detect-

TABLE 2 Cohorts of HLA-A*02:01-positive, HSV-seropositive SYMP and ASYMP individuals enrolled in the study[a]

Characteristic	Result for all subjects (n = 781)
No. (%) of subjects by gender	
Female	395 (51)
Male	386 (49)
No. (%) of subjects by race	
White	543 (69)
Nonwhite	238 (31)
Median (range) age (yr)	30 (21–67)
No. (%) of subjects by HSV infection status	
HSV-1 positive	283 (36)
HSV-2 positive	366 (47)
HSV-1 and HSV-2 positive	31 (4)
HSV negative	92 (12)
No. (%) of subjects by HLA-A*02:01 status	
Positive	411 (53)
Negative	370 (44)
No. (%) of subjects by herpes disease status	
ASYMP	711 (91)
SYMP	70 (9)

[a]The definitions of SYMP and ASYMP individuals are detailed in Materials and Methods.

able levels of any clinical herpes disease and (ii) 10 symptomatic (SYMP) patients with a history of numerous episodes of well-documented recurrent clinical herpesvirus diseases, such as herpetic lid lesions, herpetic conjunctivitis, dendritic or geographic keratitis, stromal keratitis, and iritis consistent with rHSK, at a frequency of 1 or more episodes per year for the past 2 years. None of the SYMP patients were on acyclovir or other antiviral or anti-inflammatory drug treatments at the time of blood sample collection. Detailed characteristics of the SYMP and ASYMP study populations used in the present study with respect to age, gender, HLA-A*02:01 frequency distribution, HSV-1 and HSV-2 seropositivity, and ocular herpetic disease status are presented in Table 2 and in the Materials and Methods. Since HSV-1 is the main cause of ocular herpes, only individuals who were HSV-1 seropositive and HSV-2 seronegative were enrolled in the present study.

We compared the frequency of CD8+ T cells specific to each of the 10 VP13/14 peptide epitopes, using HLA-A*02:01-specific tetramers and anti-CD8 monoclonal antibodies (MAbs), in the peripheral blood of 10 HLA-A*02:01-positive, HSV-1-seropositive ASYMP individuals and 10 HLA-A*02:01-positive, HSV-1-seropositive SYMP individuals, as described above (Fig. 1). Tetramers specific to all the 10 peptides were tested regardless of their affinity of binding to HLA-A*02:01 molecules because the lack of binding may not always translate into a lack of frequency or function (4, 15). The low frequencies of peripheral blood mononuclear cell (PBMC)-derived HSV-specific CD8+ T cells complicate direct *ex vivo* detection with tetramers using a typical number of PBMCs ($\sim 10^6$ cells). Additionally, a prior expansion of CD8+ T cells by HSV-1 or peptide stimulation in an *in vitro* culture would hamper a reliable determination of the frequency, phenotype, and function of epitope-specific CD8+ T cells. We therefore opted to measure the frequencies of VP13/14 epitope-specific CD8+ T cells *ex vivo* using 10 times the number of PBMCs ($\sim 10 \times 10^6$) per tetramer and CD8 MAb panel. The representative dot plots shown in Fig. 2A indicate the detection of higher frequencies of CD8+ T cells specific to the three immunodominant VP13/$14_{286-294}$, VP13/$14_{504-512}$, and VP13/$14_{544-552}$ epitopes in one ASYMP individual (Fig. 2A, top) than one SYMP individual (Fig. 2A, bottom). Figure 2B shows the median frequencies detected in 10 SYMP individuals and 10 ASYMP individuals. The frequencies of tetramer-positive

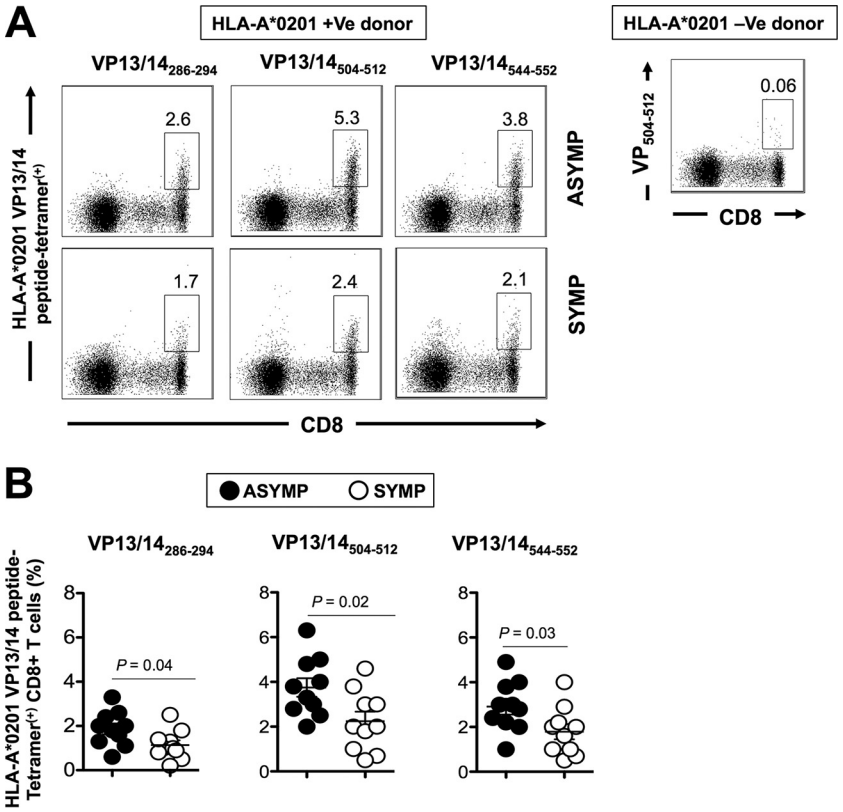

FIG 2 CD8$^+$ T cells specific to VP13/14$_{286-294}$, VP13/14$_{504-512}$, and VP13/14$_{544-552}$ epitopes are detected at higher frequencies in ASYMP than in SYMP individuals. PBMCs ($\sim$10 $\times$ 10^6) derived from 10 HLA-A*02:01-positive, HSV-1-seropositive ASYMP individuals and from 10 HLA-A*02:01-positive, HSV-1-seropositive SYMP individuals were analyzed *ex vivo* by FACS for the frequency of CD8$^+$ T cells specific to three VP13/14 epitopes using HLA-A*02:01 VP13/14 peptide-tetramer complexes representing each of the three peptides with medium to high levels of binding (VP13/14$_{286-294}$, VP13/14$_{504-512}$, and VP13/14$_{544-552}$ epitopes), as determined in the assay whose results are presented in Fig. 1. (A) Representative FACS data on the frequencies of CD8$^+$ T cells specific to the VP13/14$_{286-294}$, VP13/14$_{504-512}$, and VP13/14$_{544-552}$ epitopes detected in PBMCs from one ASYMP individual (top) and one SYMP individual (bottom). +Ve, positive; –Ve, negative. Values within the panels represent percentages of VP13/14 epitope-specific CD8$^+$ T cells. (B) Average frequencies of PBMC-derived CD8$^+$ T cells specific to VP13/14$_{286-294}$, VP13/14$_{504-512}$, and VP13/14$_{544-552}$ epitopes detected from 10 ASYMP individuals and 10 SYMP individuals. The results are representative of those from 2 independent experiments. The indicated *P* values, calculated using an unpaired *t* test, show statistically significant differences between SYMP and ASYMP individuals.

CD8$^+$ T cells specific to the VP13/14$_{286-294}$, VP13/14$_{504-512}$, and VP13/14$_{544-552}$ epitopes that were consistently detected in both SYMP and ASYMP individuals were recorded and ranged from 1.7% to 5.3%. Significantly higher frequencies of CD8$^+$ T cells specific to the VP13/14$_{286-294}$, VP13/14$_{504-512}$, and VP13/14$_{544-552}$ epitopes were detected in ASYMP individuals than SYMP individuals ($P = 0.042$, $P = 0.02$, and $P = 0.035$, respectively). Despite repeated attempts with and without *in vitro* expansions, the remaining seven VP13/14 peptide and HLA-A*02:01 tetramers consistently detected CD8$^+$ T cells in HLA-A*02:01-positive, HSV-seropositive SYMP and ASYMP individuals at a low and nonsignificant frequency (data not shown).

Altogether, the results indicate that although CD8$^+$ T cells from both ASYMP and SYMP individuals frequently recognized the VP13/14$_{286-294}$,VP13/14$_{504-512}$, and VP13/14$_{544-552}$ epitopes, there was a significantly higher frequency of recognition by CD8$^+$ T cells from ASYMP individuals than SYMP individuals.

VP13/14 epitope-specific CD8$^+$ T$_{EM}$ cells correlate with asymptomatic individuals, while VP13/14 epitope-specific CD8$^+$ T$_{CM}$ cells correlate with symptomatic individuals. We next determined whether the VP13/14$_{286-294}$, VP13/14$_{504-512}$, and VP13/14$_{544-552}$ epitope-specific memory CD8$^+$ T cells contain distinct subpopulations

of central memory T cells (T_{CM} cells) and effector memory T cells (T_{EM} cells). T_{CM} cells are characterized by the differential expression of L-selectin CD62L and chemokine receptor CCR7; however, T_{EM} cells are memory cells that have lost the constitutive expression of CCR7 and CD62L (2, 4, 14, 36). ASYMP individuals had significantly higher percentages of CD44^{high} CC62L^{low} CD8$^+$ T_{EM} cells specific to the VP13/14$_{286-294}$ (Fig. 3A, and B), VP13/14$_{504-512}$ (Fig. 3C and D), and VP13/14$_{544-552}$ (Fig. 3E and F) epitopes than SYMP individuals ($P < 0.05$, unpaired *t* test). In contrast, significantly higher percentages of VP13/14$_{286-294}$, VP13/14$_{504-512}$, and VP13/14$_{544-552}$ epitope-specific CD8$^+$ CD44^{high} CC62L^{high} T_{CM} cells were consistently detected in SYMP individuals than ASYMP individuals ($P < 0.01$, unpaired *t* test).

Using other differentiation markers, CD45RA and chemokine receptor CCR7, to phenotype CD8$^+$ T_{EM}- and T_{CM}-cell subpopulations, we found that ASYMP individuals had significantly higher percentages of CD45RA$^-$ CCR7$^-$ CD8$^+$ T_{EM} cells specific to VP13/14$_{286-294}$ (Fig. 3G and H), VP13/14$_{504-512}$ (Fig. 3I and J), and VP13/14$_{544-552}$ (Fig. 3K and L) epitopes, while SYMP individuals had significantly higher percentages of CD45RA$^-$ CCR7$^+$ CD8$^+$ T_{CM} cells ($P < 0.05$, unpaired *t* test). The T_{EM}- and T_{CM}-cell phenotypes of enriched CD8$^+$ T cells were also compared following *in vitro* stimulation with either SYMP or ASYMP peptides. As expected, there was an increase in the CD8$^+$ T_{EM}-cell population in cells stimulated *in vitro* with ASYMP epitopes. In contrast, there was an increase in the CD8$^+$ T_{CM}-cell population in cells stimulated *in vitro* with SYMP epitopes (see Fig. S2 in the supplemental material).

Overall, four main CD8$^+$ T-cell subpopulations were identified on the basis of the expression of CD45RA and CCR7: conventional T_{EM} (CD45RA$^-$ CCR7$^-$) and T_{CM} (CD45RA$^-$ CCR7$^+$) cells, the newly described memory CD45RA$^+$ CCR7$^+$ T cells with a naive phenotype (T_{MNP}), and CD45RA$^+$ CCR7$^-$ T_{EMRA} (CD45RA$^+$ effector memory) cells (37). Similar frequencies of CD45RA$^+$ CCR7$^+$ T_{MNP} cells were detected in SYMP and ASYMP individuals. However, CD45RA$^+$ CCR7$^-$ CD8$^+$ T_{EMRA} cells appeared to be predominant in ASYMP individuals but not in SYMP individuals (Fig. 3G, I, and K).

Altogether, the phenotypic properties of HSV-1 VP13/14 epitope-specific memory CD8$^+$ T cells revealed a clear dichotomy in HSV-specific memory CD8$^+$ T-cell subpopulations, with ASYMP individuals featuring higher frequencies of CD8$^+$ T_{EM} cells and SYMP individuals featuring higher frequencies of CD8$^+$ T_{CM} cells. Thus, the results suggest that at a second pathogen encounter (e.g., following HSV-1 reactivation from latency or reinfection), ASYMP individuals but not SYMP individuals would better contain the herpesvirus infection and disease by mounting faster and stronger protective HSV-specific CD8$^+$ T_{EM}-cell responses.

Polyfunctional VP13/14-specific CD8$^+$ T cells are associated with asymptomatic herpes. We compared the levels of granzyme B (GzmB), granzyme K (GzmK), and perforin (PFN) expressed on gated VP13/14$_{286-294}$, VP13/14$_{504-512}$, and VP13/14$_{544-552}$ epitope-specific CD8$^+$ T cells from 10 SYMP and 10 ASYMP individuals (Fig. 4A and B). We found that higher levels of GzmB, GzmK, and PFN were expressed on VP13/14$_{286-294}$, VP13/14$_{504-512}$, and VP13/14$_{544-552}$ epitope-specific CD8$^+$ T cells from ASYMP individuals than on those from SYMP individuals. This indicates a positive correlation of VP13/14-specific CD8$^+$ T-cell cytotoxic function with protection against ocular herpetic disease.

We next assessed whether VP13/14 epitope-specific CD8$^+$ T cells display cytotoxic activity. Fresh PBMC-derived CD8$^+$ T-cell lines were generated from HLA-A*02:01-positive ASYMP and SYMP individuals following *in vitro* stimulation with individual VP13/14$_{286-294}$, VP13/14$_{504-512}$, and VP13/14$_{544-552}$ epitope peptides. The cytotoxicity was measured by detecting the level of CD107$^{a/b}$ expression by fluorescence-activated cell sorting (FACS) on gated CD8$^+$ T cells. CD107^a and CD107^b are lysosome-associated membrane glycoproteins that surround the core of the lytic granules (4, 38). Upon engagement with the T-cell receptor and epitope stimulation, CD107$^{a/b}$ are exposed on the cell membrane of CD8$^+$ cytotoxic T lymphocytes (CTLs). Thus, the level of CD107$^{a/b}$ expression on the surface of CTLs is used as a direct assay for the human epitope-specific CTL response (38). As shown in Fig. 4C to E, a higher percentage of VP13/

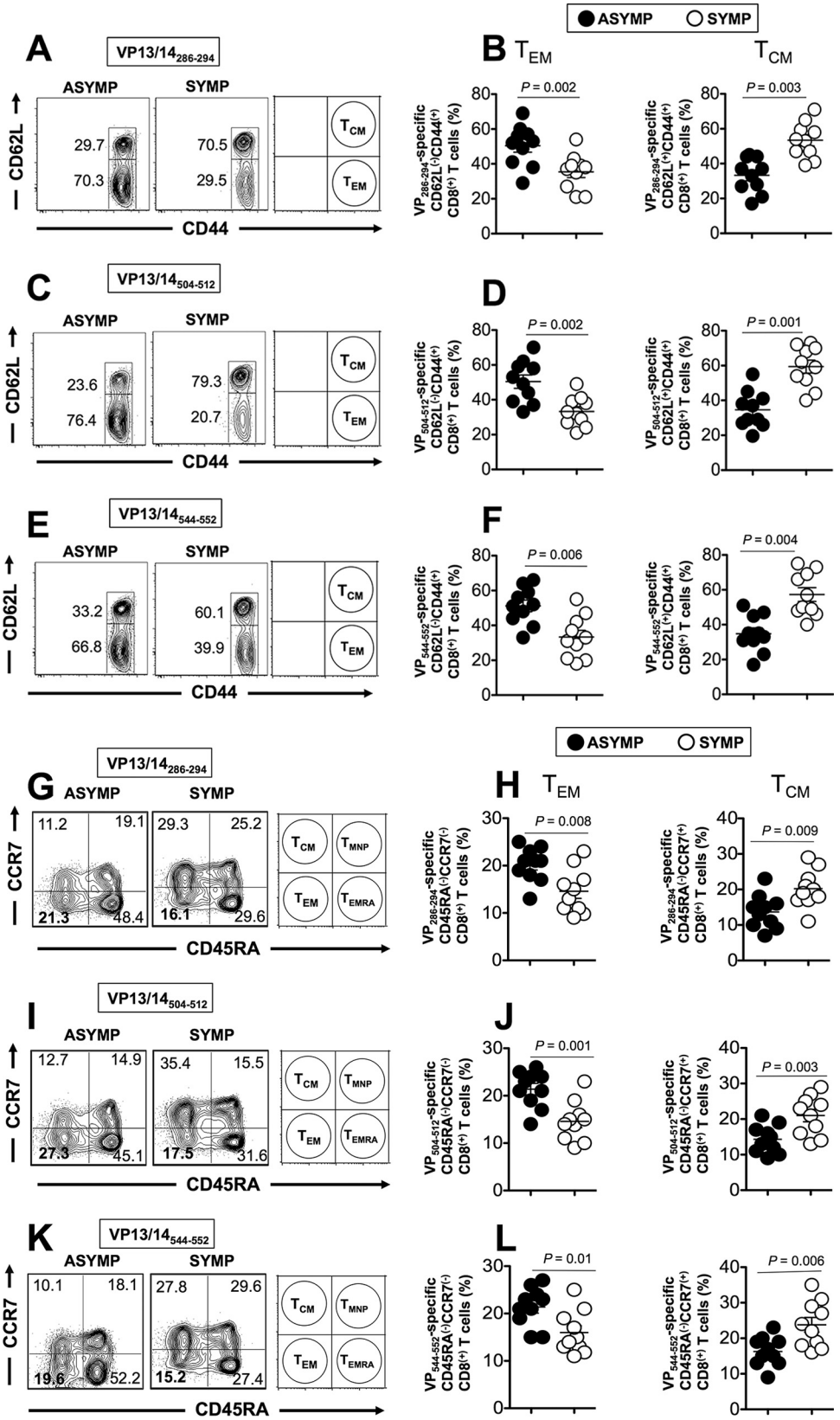

FIG 3 More VP13/14 epitope-specific CD44^{high} CD62L^{low} CD8$^+$ T_{EM} cells are detected in ASYMP individuals than in SYMP individuals. The T_{EM}- and T_{CM}-cell phenotypes of CD8$^+$ T cells specific to VP13/14$_{286-294}$, VP13/14$_{504-512}$, and VP13/14$_{544-552}$ epitopes among PBMCs of 10 HLA-A*02:01-positive, HSV-1-seropositive SYMP individuals and 10 HLA-A*02:01-positive, HSV-1-seropositive ASYMP individuals were analyzed by FACS. (A, C, and E) Representative FACS data on the frequencies of CD44^{high} CD62L^{low} CD8$^+$ T_{EM} cells and CD44^{high} CD62L^{high} CD8$^+$ T_{CM} cells in PBMCs

(Continued on next page)

$14_{286-294}$, VP13/$14_{504-512}$, and VP13/$14_{544-552}$ epitope-specific CD8$^+$ T cells from ASYMP individuals expressed detectable levels of CD107$^{a/b}$. In contrast, fewer VP13/$14_{286-294}$, VP13/$14_{504-512}$, and VP13/$14_{544-552}$ epitope-specific CD8$^+$ T cells from SYMP patients expressed CD107$^{a/b}$. As expected, no significant percentage of CD8$^+$ T cells upregulated CD107$^{a/b}$ after incubation with mock-infected or target cells (data not shown).

The levels of the interleukin-2 (IL-2) and tumor necrosis factor alpha (TNF-α) effector cytokines produced by T cells from ASYMP and SYMP individuals following *in vitro* stimulation with VP13/14 peptides were determined. As shown in Fig. 4F and G, VP13/$14_{504-512}$ and VP13/$14_{544-552}$ epitope-specific CD8$^+$ T cells from ASYMP individuals produced significantly more IL-2 and TNF-α than such CD8$^+$ T cells from SYMP patients ($P < 0.05$).

We next determined the ability of VP13/14 epitopes to stimulate the production of gamma interferon (IFN-γ) by CD8$^+$ T cells from SYMP and ASYMP individuals. Freshly isolated CD8$^+$ T cells from SYMP and ASYMP individuals were stimulated *in vitro* for 6 h with individual VP13/$14_{286-294}$, VP13/$14_{504-512}$, and VP13/$14_{544-552}$ epitope peptides, as described in Materials and Methods. The percentage and number of IFN-γ-producing CD8$^+$ T cells from SYMP and ASYMP individuals were compared by intracellular FACS staining. Significantly higher percentages of VP13/$14_{286-294}$, VP13/$14_{504-512}$, and VP13/$14_{544-552}$ epitope-specific IFN-γ-producing CD8$^+$ T cells were detected in ASYMP individuals than SYMP individuals ($P < 0.05$) (Fig. 4H to J). Overall, the results presented above indicate that VP13/14-specific CD8$^+$ T cells from ASYMP individuals (i) have higher levels of cytotoxic activity than CD8$^+$ T cells from SYMP patients and (ii) have cytotoxic activity against HSV-1-infected cells.

The percentage of SYMP and ASYMP individuals that showed significant results for one or several CD8$^+$ T-cell functions are summarized in Fig. 4K. Overall, 86% of ASYMP individuals had VP13/14-specific CD8$^+$ T cells with three to five functions, indicating their ability to display concurrent polyfunctional activities: (i) production of high levels of GzmB, (ii) production of high levels of GzmK, (iii) production of high levels of perforin, (iv) expression of high levels of CD107$^{a/b}$ lytic granules (cytotoxic activity), and (v) production of high levels of IFN-γ. In contrast, only 42% of SYMP patients had VP13/14-specific CD8$^+$ T cells with three functions, while the majority of SYMP patients had VP13/14-specific CD8$^+$ T cells with just one or two functions.

To further compare the HSV-specific CD8$^+$ T-cell function between SYMP and ASYMP individuals, we studied the expression of Ki-67 on VP13/14 epitope-specific CD8$^+$ T cells. Higher frequencies of VP13/$14_{504-512}$-specific Ki-67 cells were detected from ASYMP individuals than SYMP individuals (Fig. 5A and B). We also analyzed the expression of PD-1, a marker of T-cell exhaustion (39). As shown in Fig. 5C and D, SYMP patients exhibited higher frequencies of VP13/$14_{504-512}$-specific PD-1-positive CD8$^+$ T cells than ASYMP individuals, suggesting functional exhaustion of HSV-specific effector CD8$^+$ T cells from SYMP patients.

To assess the differentiation status of HSV-specific CD8$^+$ T cells from SYMP versus ASYMP individuals, we compared the expression patterns of eomesodermin (Eomes) and T-bet transcription factors *ex vivo* on CD8$^+$ T cells from SYMP and ASYMP individuals at both the mRNA level (using reverse transcription-PCR [RT-PCR]) and the protein level (using FACS). Eomes and T-bet are T-box transcription factors that are expressed in activated CD8$^+$ T cells. Eomes and T-bet function as a molecular switch between T_{CM}- and T_{EM}-cell differentiation by driving the differentiation of CD8$^+$ T_{EM}

FIG 3 Legend (Continued)
from one SYMP individual and one ASYMP individual. (B, D, and F) Average frequencies of VP13/14-specific T_{EM} or T_{CM} CD8$^+$ T cells from 10 SYMP and 10 ASYMP individuals. (G, I, and K) Representative FACS data on the frequencies of CD8$^+$ CD45RA$^-$ CCR7$^-$ T_{EM} cells and CD8$^+$ CD45RA$^-$ CCR7$^+$ T_{CM} cells in one ASYMP individual and one SYMP individual. (H, J, and L) Average frequencies of VP13/14-specific T_{EM} and T_{CM} CD8$^+$ cells from 10 ASYMP and 10 SYMP individuals. The results are representative of those from 2 independent experiments. The indicated *P* values, calculated using an unpaired *t* test, show statistically significant differences between ASYMP and SYMP individuals.

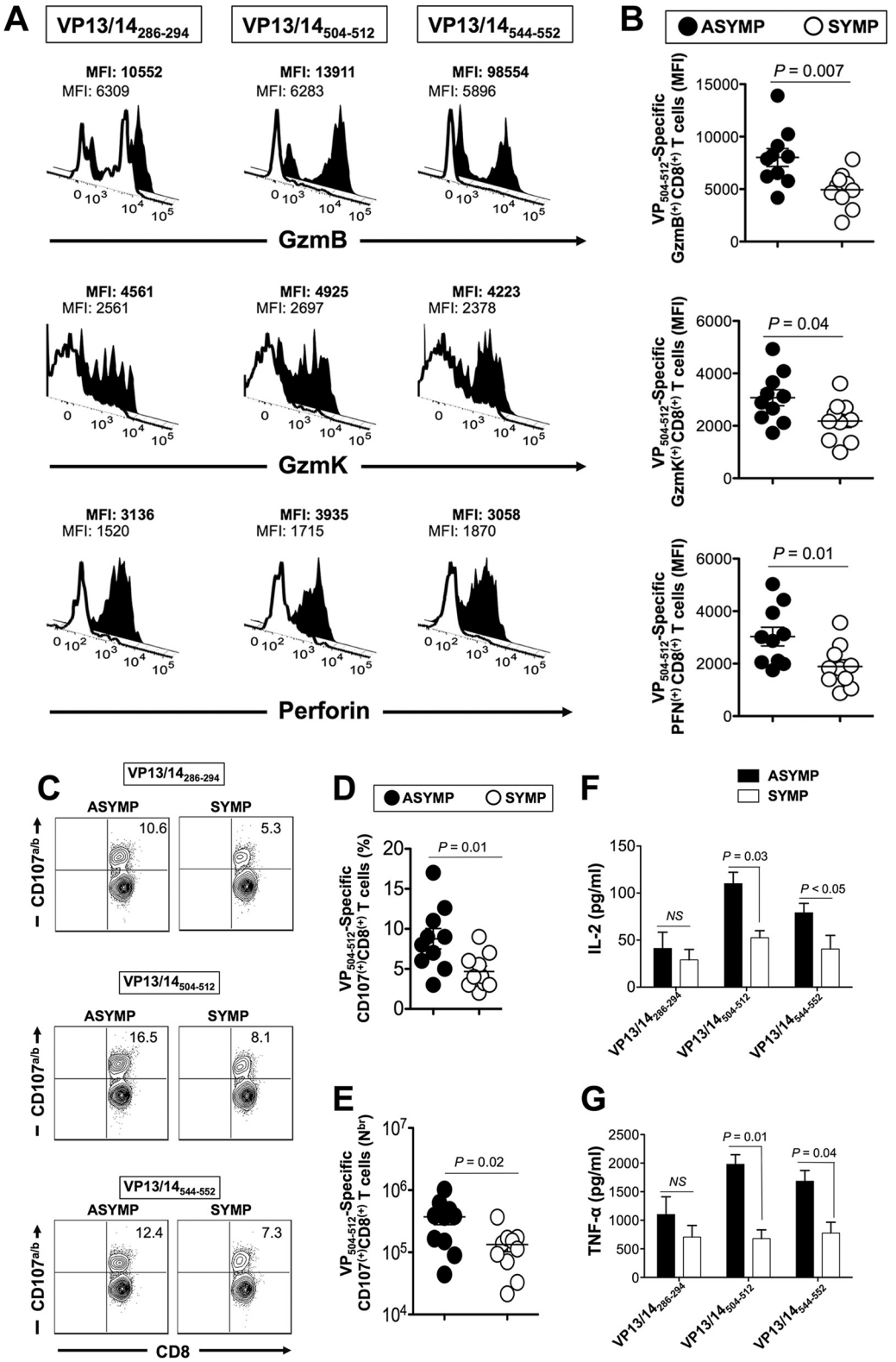

FIG 4 Higher proportions of polyfunctional HSV-1 VP13/14 epitope-specific CD8$^+$ T cells are detected in asymptomatic individuals. (A) Representative FACS data on the levels expression of GzmB, GzmK, and PFN on tetramer-gated CD8$^+$ T cells specific for the VP13/14$_{286-294}$, VP13/14$_{504-512}$, and VP13/14$_{544-552}$ epitopes, determined by FACS. Samples were acquired on a BD LSRII flow cytometer, and data analysis was performed using FlowJo software. The numbers on the top of each histogram represent MFIs, depicting the level of expression of each cytotoxic molecule. Numbers in bold represent the MFIs for ASYMP individuals, and numbers in nonbold represent the MFIs for SYMP individuals. (B) Average MFI for the

(Continued on next page)

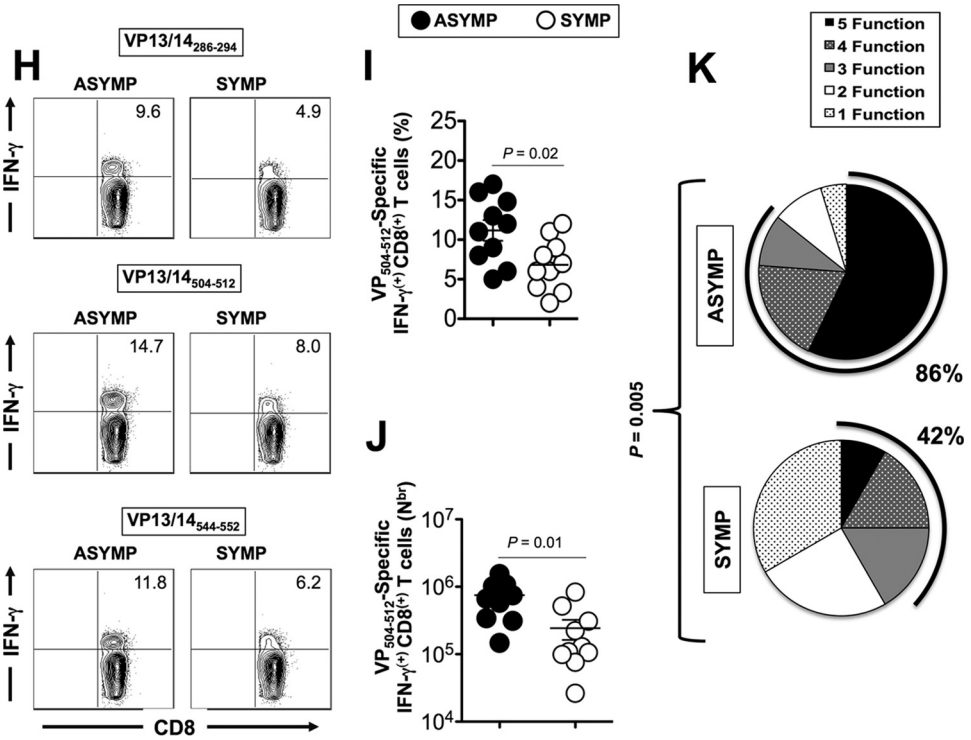

FIG 4 Legend (Continued)

levels of VP13/$14_{504-512}$ epitope-specific GzmB, GzmK, and PFN expression for 10 ASYMP and 10 SYMP individuals. (C) Representative FACS data on VP13/$14_{286-294}$, VP13/$14_{504-512}$, and VP13/$14_{544-552}$ epitope-specific CD107$^{a/b high}$ CD8$^+$ T cells from one ASYMP individuals and one SYMP individual. (D and E) Average percentage (D) and average absolute number (N^{br}) (E) of VP13/$14_{504-512}$ epitope-specific CD107a/b^{high} CD8$^+$ T cells from 10 ASYMP and 10 SYMP individuals. (F and G) Average amounts of IL-2 (F) and TNF-α (G) effector cytokines produced by CD8$^+$ T cells from ASYMP and SYMP individuals, as detected by the Luminex assay. (H) Representative FACS data for VP13/$14_{286-294}$, VP13/$14_{504-512}$, and VP13/$14_{544-552}$ epitope-specific IFN-γ^{high} CD8$^+$ T cells from one ASYMP individual and one SYMP individual. (I and J) Average percentage (I) and average absolute number (J) of VP13/$14_{504-512}$ epitope-specific IFN-γ^{high} CD8$^+$ T cells from 10 ASYMP and 10 SYMP individuals. (K) Pie charts representing the overall mean number of CD8$^+$ T-cell functions detected from 10 ASYMP and 10 SYMP individuals in response to stimulation with VP13/14 peptides. The results are representative of those from 2 independent experiments. The indicated *P* values, calculated using an unpaired *t* test, show statistically significant differences between ASYMP and SYMP individuals. NS, no significant difference.

cells at the expense of T_{CM} cells (40–44). As shown in Fig. 5E to G, a significantly higher proportion of VP13/$14_{504-512}$-specific CD8$^+$ T cells from ASYMP individuals than VP13/$14_{504-512}$-specific CD8$^+$ T cells from SYMP individuals expressed Eomes at the RNA level (as determined using RT-PCR) (Fig. 5E). Furthermore, a higher proportion of VP13/$14_{504-512}$-specific CD8$^+$ T cells from ASYMP individuals than SYMP individuals was Eomes^{high} ($P < 0.001$) (Fig. 5F and G). Similar results were obtained when the expression of T-bet in VP13/14 CD8$^+$ T cells from SYMP and ASYMP individuals was analyzed (Fig. 5H to J).

Altogether, the results indicate that the VP13/14-specific CD8$^+$ T-cell responses associated with the control of herpes disease differ in ASYMP and SYMP individuals: (i) increases in IFN-γ and Ki-67 levels and the cytolytic activity of VP13/14-epitope specific CD8$^+$ T cells from ASYMP individuals are all characteristics of less differentiated effector T cells; (ii) the high levels of expression of the PD-1 exhaustion marker on HSV-1 VP13/14-specific effector CD8$^+$ T cells from SYMP individuals suggest a total or partial dysfunctionality; (iii) the higher levels of expression of Eomes and T-bet by CD8$^+$ T cells from ASYMP individuals may favor an effector-to-memory CD8$^+$ T-cell transition (E $\rightarrow$ M) and the formation of a higher percentage of CD8$^+$ T_{EM} cells, as seen in ASYMP individuals (45); and (iv) ASYMP individuals had mostly multifunctional CD8$^+$ T cells with the simultaneous expression of three to five functions, whereas SYMP individuals had a majority of CD8$^+$ T cells with just one or two simultaneous functions.

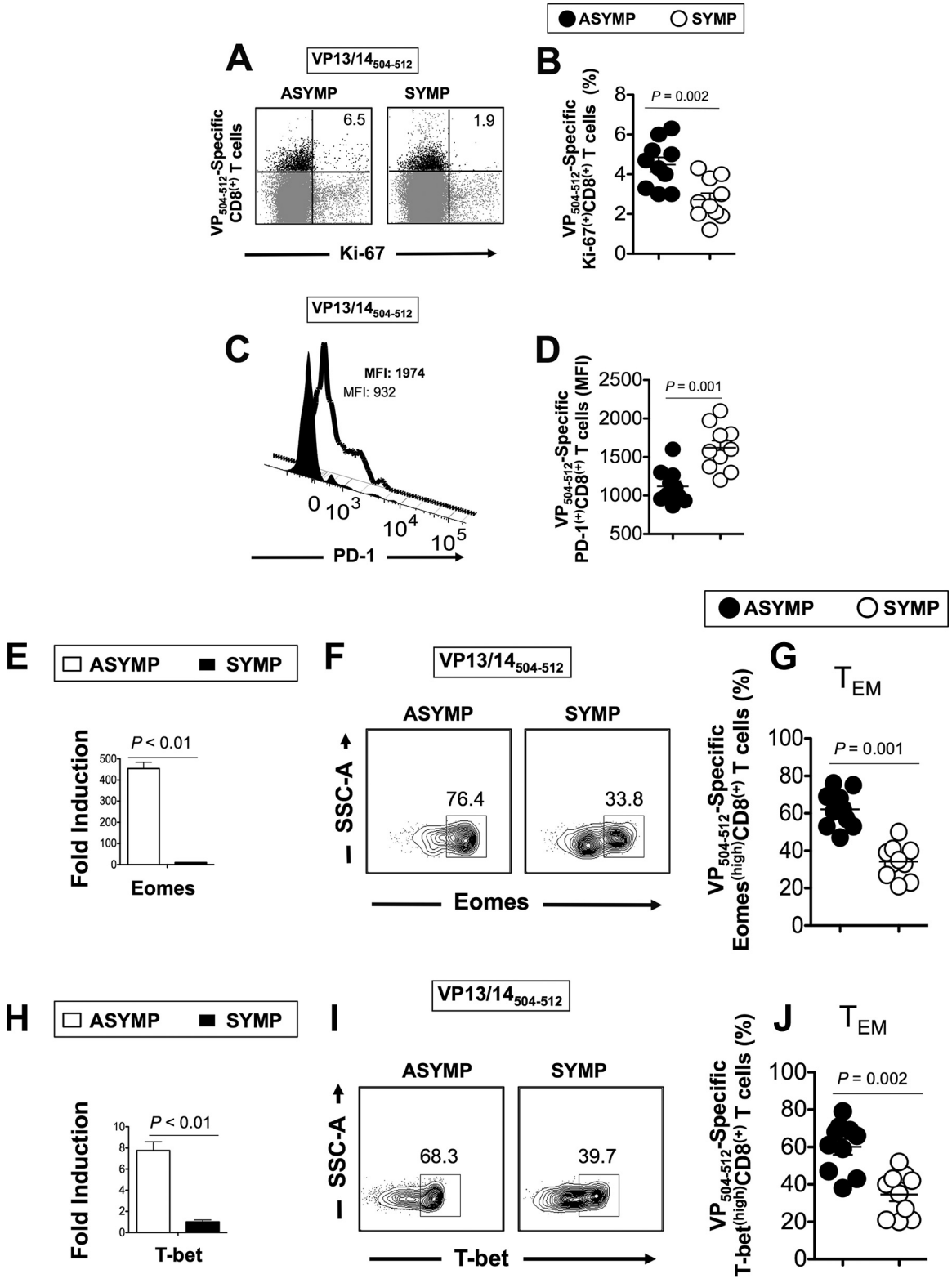

FIG 5 Asymptomatic individuals had a significantly higher proportion of differentiated and functional VP13/14 epitope-specific $CD8^+$ T cells. (A and B) Representative FACS data (A) and average frequencies (B) of $VP_{504-512}$-specific Ki-67-positive [Ki-$67^{(+)}$] $CD8^+$ T cells from 10 ASYMP and 10 SYMP individuals. (C) Representative histograms showing the numbers of $VP_{504-512}$-specific PD-1^{high} $CD8^+$ T cells from one ASYMP individual (closed histogram and nonbold data) and one SYMP individual (open histogram and bold data). (D) Average frequencies of $VP_{504-512}$-specific PD-1^{high} $CD8^+$ T cells from 10 ASYMP and 10 SYMP individuals. (E and H) The expression patterns of the T-bet (H) and Eomes (E) transcription factors from $CD8^+$ T cells derived from SYMP and ASYMP individuals were analyzed at the RNA level, using RT-PCR. (F and I) Representative FACS data on the percentage of Eomes-positive (F) and T-bet-positive (I) HSV-1 VP13/$14_{504-512}$-specific $CD8^+$ T cells derived from one SYMP individual and one ASYMP individual. SSC, side scatter. (G and J) Average frequencies of the

(Continued on next page)

Immunization with VP13/14 epitopes that are highly recognized by CD8$^+$ T_{EM} cells from asymptomatic individuals elicited a strong protective immunity against ocular herpes in HLA-A*02:01 transgenic mice. We next evaluated whether immunization with ASYMP CD8$^+$ T_{EM}-cell epitopes (i.e., VP13/14$_{286-294}$, VP13/14$_{504-512}$, and VP13/14$_{544-552}$) confers protection against ocular herpes using our established susceptible humanized HLA-A*02:01 transgenic mouse model (HLA Tg mice on a BALB/c mouse genetic background) (4).

Three groups of HLA Tg mice ($n = 10$ mice per group) were immunized subcutaneously twice with a 21-day interval with a mixture of ASYMP CD8$^+$ T-cell human epitopes (VP13/14$_{286-294}$, VP13/14$_{504-512}$, and VP13/14$_{544-552}$) or a mixture of SYMP CD8$^+$ T-cell human epitopes (VP13/14$_{410-418}$, VP13/14$_{497-505}$, and VP13/14$_{657-665}$) delivered as a mixture with the CD4$^+$ T-cell PADRE epitope emulsified in CpG_{1826} adjuvant. These mice are referred to here as ASYMP and SYMP mice, respectively. Control (mock-vaccinated) mice received CpG_{1826} adjuvant alone. Two weeks after the second and final immunization, animals from both the vaccinated and mock-vaccinated groups received an ocular HSV-1 challenge (2×10^5 PFU of the McKrae strain without scarification). The mice were then assessed for up to 30 days postchallenge for ocular herpes disease, ocular viral titers, and survival.

As shown in Fig. 6A and B, significantly lower clinical scores of ocular herpes disease were observed in mice immunized with ASYMP epitopes (group 1) than mice immunized with the SYMP epitopes (group 2) and mock-immunized mice ($P = 0.02$ and $P = 0.004$, respectively). Furthermore, significantly fewer virus particles were detected on day 7 postinfection (the peak of viral replication) in eye swab specimens from the ASYMP group than in eye swab specimens from the SYMP group and the mock-immunized group ($P = 0.03$ and $P = 0.003$, respectively) (Fig. 6C). Seventy percent of the animals in the ASYMP group survived the infection, whereas only 30% of the animals in the SYMP group and 10% of the animals in the mock-immunized group survived the infection ($P < 0.05$) (Fig. 6D).

We next determined the phenotype of CD8$^+$ T cells from the corneas of the protected ASYMP group, the nonprotected SYMP group, and the mock-immunized group. For simplicity, only the extreme scores for ASYMP and SYMP mice were used in these studies. Thus, SYMP mice had a clinical score of $\geq$3. ASYMP mice had a clinical score of $\leq$1.0. As shown in Fig. 6E and F, protected ASYMP mice had significantly more cornea-resident CD44^{high} CD62L^{low} CD8$^+$ T_{EM} cells than nonprotected SYMP and mock-immunized mice ($P = 0.03$ and $P = 0.05$, respectively). In contrast, significantly more cornea-resident CD44^{high} CD62L^{high} CD8$^+$ T_{CM} cells were detected in SYMP and mock-immunized mice than ASYMP mice ($P = 0.04$) (Fig. 6E and F).

Altogether, these results indicate that vaccination with ASYMP HSV-1 VP13/14$_{286-294}$, VP13/14$_{504-512}$, and VP13/14$_{544-552}$ peptide epitope-specific CD8$^+$ T_{EM} cells decreased the level of ocular herpesvirus infection and disease and protected against death in susceptible HLA Tg mice. These results also indicate that cornea-resident VP13/14-specific CD8$^+$ T_{EM} cells are associated with protection from ocular herpes.

Frequent VP13/14-specific CD8$^+$ T_{EM} cells are detected in the corneas of HSV-1-infected ASYMP HLA transgenic mice. We next determined the phenotype and function of VP13/14-specific CD8$^+$ T cells from the corneas of infected (nonvaccinated) SYMP versus ASYMP HLA Tg mice. Mice were infected and then segregated into ASYMP and SYMP groups on the basis of the clinical score of their ocular herpetic disease. As shown in Fig. 7A to F, ASYMP mice had significantly more cornea-resident VP13/14$_{286-294}$, VP13/14$_{504-512}$, and VP13/14$_{544-552}$ epitope-specific CD44^{high} CD62L^{low} CD8$^+$ T_{EM} cells than SYMP mice (88.5% versus 75.4%, 83.3% versus 69.1%

FIG 5 Legend (Continued)
expression patterns of the Eomes (G) and T-bet (J) transcription factors at the protein level from gated VP13/14$_{504-512}$-specific CD8$^+$ T_{EM} cells derived from 10 SYMP and 10 ASYMP individuals analyzed by FACS. The results are representative of those from 3 independent experiments. The indicated *P* values, calculated using an unpaired *t* test, show statistically significant differences between SYMP and ASYMP individuals.

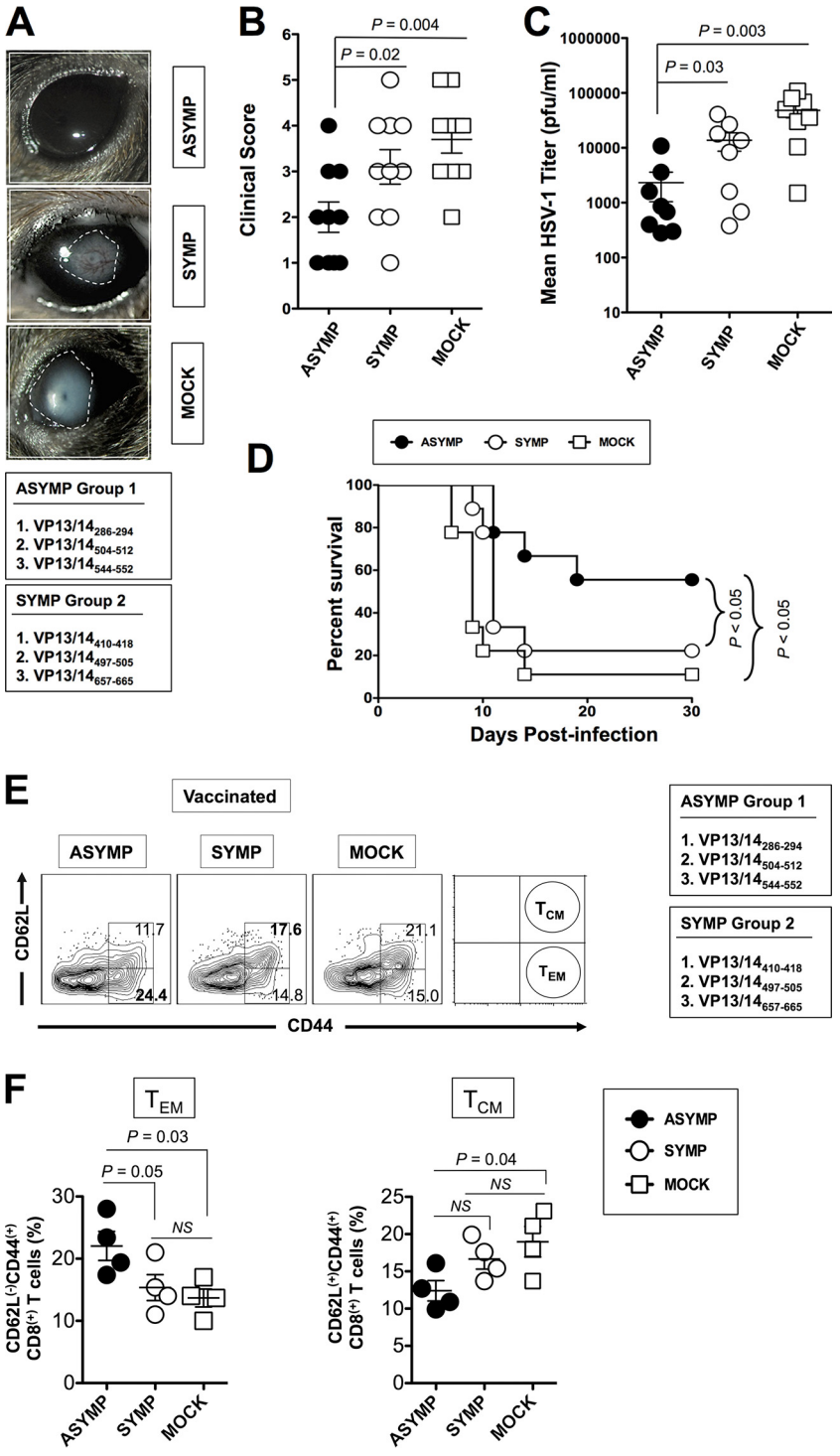

FIG 6 Protective immunity against ocular herpes induced by ASYMP VP13/14 $CD8^+$ T_{EM}-cell epitopes in humanized HLA transgenic mice. Three groups of age- and sex-matched HLA Tg mice ($n = 10$ each) were immunized subcutaneously on days 0 and 21 with a mixture of ASYMP $CD8^+$ T-cell peptide epitopes ($VP13/14_{286-294}$, $VP13/14_{504-512}$, and $VP13/14_{544-552}$) and a mixture of SYMP $CD8^+$ T-cell human epitopes ($VP13/14_{410-418}$, $VP13/14_{497-505}$ and $VP13/14_{657-665}$). These were delivered together with a promiscuous $CD4^+$ T-cell epitope (PADRE) emulsified in CpG_{1826} adjuvant. CpG_{1826} adjuvant alone was used for mock vaccination. Two weeks after the final immunization, all animals were challenged ocularly with 2×10^5 PFU of HSV-1 (strain McKrae). (A and B) The severity of herpetic eye disease was followed for 2 weeks after immunization and scored on a scale of from 1 to 5. (C) Virus titrations were determined from eye swab specimens collected on day 7 postinfection. (D) Survival was determined within a window of 30 days postchallenge. Corneas were harvested from each group, and the frequencies of $CD44^{high}$ $CD62L^{low}$ $CD8^+$ T_{EM} cells and $CD44^{high}$ $CD62L^{high}$ $CD8^+$ T_{CM} cells were analyzed by FACS using specific MAbs. (E)

(Continued on next page)

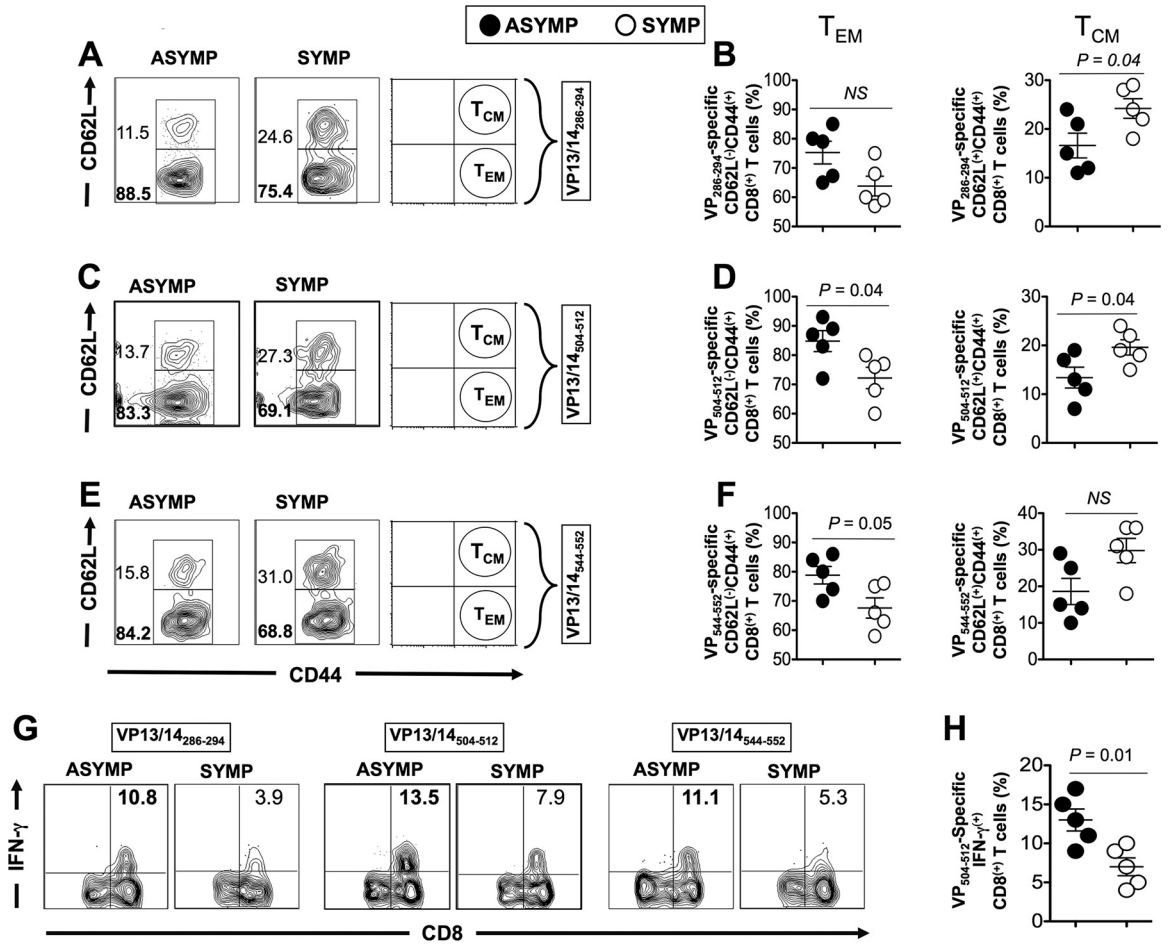

FIG 7 The corneas of protected ASYMP HLA transgenic mice have more VP13/14-specific polyfunctional CD8+ T_{EM} cells than the corneas of nonprotected SYMP mice. Mice were infected with HSV-1 and then segregated into two groups, (i) ASYMP mice and (ii) SYMP mice, on the basis of the clinical score for their ocular herpetic disease. Corneas were harvested from each group on day 9 postinfection, and the frequencies of $CD44^{high}$ $CD62L^{low}$ CD8+ T_{EM} cells and $CD44^{high}$ $CD62L^{high}$ CD8+ T_{CM} cells specific to the $VP13/14_{286-294}$, $VP13/14_{504-512}$, and $VP13/14_{544-552}$ epitopes were analyzed by FACS using tetramers and specific MAbs, as described in Materials and Methods. (A, C, and E) Representative data on the frequencies of $VP13/14_{286-294}$-specific (A), $VP13/14_{504-512}$-specific (C), and $VP13/14_{544-552}$-specific (E) T_{EM} cells and CD8+ T_{CM} cells detected from the corneas of one ASYMP HLA Tg mouse and one SYMP HLA Tg mouse. (B, D, and F) Average frequencies of $VP13/14_{286-294}$-specific (B), $VP13/14_{504-512}$- specific (D), and $VP13/14_{544-552}$-specific (F) T_{CM} and T_{EM} CD8+ cells detected in the corneas of five ASYMP HLA Tg mice and five SYMP HLA Tg mice. (G) Representative data on the percentage of IFN-γ-positive CD8+ T cells specific to $VP13/14_{286-294}$, $VP13/14_{504-512}$, and $VP13/14_{544-552}$ epitopes detected from ASYMP and SYMP mice. (H) Average frequencies of IFN-γ-positive CD8+ T cells specific to the $VP13/14_{504-512}$ peptide. The results are representative of those from 2 independent experiments. The indicated *P* values, calculated using an unpaired *t* test, show a statistically significant difference between SYMP and ASYMP mice.

[$P = 0.04$], and 84.2% versus 68.8% [$P = 0.05$], respectively). In contrast, significantly more cornea-resident $VP13/14_{286-294}$, $VP13/14_{504-512}$, and $VP13/14_{544-552}$ epitope-specific $CD44^{high}$ $CD62L^{high}$ CD8+ T_{CM} cells were detected in SYMP mice than ASYMP mice ($P = 0.04$) (Fig. 7A to F). These results confirm that cornea-resident VP13/14-specific CD8+ T_{EM} cells are associated with protection from ocular herpes.

We next determined the ability of CD8+ T cells from SYMP versus ASYMP mice to produce IFN-γ following stimulation with $VP13/14_{286-294}$, $VP13/14_{504-512}$, and

FIG 6 Legend (Continued)

Representative data on the frequencies of CD8+ T_{EM} and CD8+ T_{CM} cells detected from the corneas of one protected ASYMP HLA Tg mouse, one nonprotected SYMP HLA Tg mouse, and one mock-immunized HLA Tg mouse. (F) Average frequencies of T_{CM} and T_{EM} CD8+ cells detected in the corneas of four ASYMP, four SYMP, and four mock-immunized HLA Tg mice. The results are representative of those from 2 independent experiments. The indicated *P* values, calculated using an unpaired *t* test, show statistically significant differences between ASYMP, SYMP, and mock-immunized mice.

VP13/14$_{544-552}$ epitope peptides. CD8$^+$ T cells were stimulated *in vitro* with individual immunodominant (VP13/14$_{286-294}$, VP13/14$_{504-512}$, and VP13/14$_{544-552}$) epitope peptides, as described in Materials and Methods. The percentages of IFN-γ-producing CD8$^+$ T cells from SYMP and ASYMP mice were compared by intracellular FACS staining. Significantly higher percentages of VP13/14$_{286-294}$, VP13/14$_{504-512}$, and VP13/14$_{544-552}$ epitope-specific CD8$^+$ T cells producing IFN-γ were detected in ASYMP mice than SYMP mice ($P = 0.01$) (Fig. 7G and H).

Altogether, the phenotypic and functional properties of HSV-1 VP13/14-specific CD8$^+$ T cells revealed that (i) the corneas of protected ASYMP HLA Tg mice but not the corneas of nonprotected SYMP mice had frequent HSV-specific CD8$^+$ T_{EM} cells and (ii) VP13/14-specific CD8$^+$ T cells from ASYMP mice displayed more concurrent functional activities than CD8$^+$ T cells from SYMP mice. The results also confirm that HLA Tg mice are a useful animal model for understanding the mechanisms by which human epitope-specific CD8$^+$ T cells mediate the control of herpes (17).

DISCUSSION

Herpes simplex virus 1 (HSV-1) is one of the most successful human pathogens, infecting up to 80% of people worldwide (2, 4, 13, 15, 20). The HSV-1-derived tegument virion phosphoproteins (VPs), which are located between the capsid and the outer viral envelope proteins, contain a large number of possible protective CD8$^+$ T-cell epitopes (11). However, only a few epitopes have been reported so far. In this study, we identified three new protective ASYMP human CD8$^+$ T_{EM}-cell epitopes from the abundant tegument VP13/14 protein: VP13/14$_{286-294}$, VP13/14$_{504-512}$, and VP13/14$_{544-552}$. These new VP13/14 epitopes displayed a high affinity of binding to purified HLA-A*02:01 molecules, stabilized HLA-A*02:01 molecules on target antigen-presenting cells (APCs), and recalled CD8$^+$ T cells in both HSV-1-seropositive ASYMP individuals and ASYMP HLA-A*02:01 transgenic mice ocularly infected with HSV-1. We additionally found that ASYMP and SYMP individuals have VP13/14 epitope-specific CD8$^+$ T cells with remarkably different phenotypes and functions. Notably, ASYMP individuals had a significantly higher proportion of differentiated polyfunctional HSV-1 VP13/14-specific CD8$^+$ T_{EM} cells. In contrast, SYMP patients had significantly higher frequencies of less differentiated monofunctional HSV-1 VP13/14-specific CD8$^+$ T_{CM} cells. Our findings provide a framework for the rational design of a herpes simplex vaccine based on epitopes that referentially induce polyfunctional CD8$^+$ T_{EM}-cell immunity.

CD8$^+$ T cells recognize their target epitopes as 8- to 10-amino-acid-long peptides which are derived from intracellular, processed viral Ags and presented by HLA class I molecules (e.g., HLA-A*02:01 molecules) expressed at the surface of infected cells (46, 47). Despite the 84-plus HSV-1 ORFs encoding hundreds of potential epitopes, protective CD8$^+$ T cells target only a few epitopes (48–51). Tegument proteins are delivered to the cytoplasm of host cells during viral entry, resulting in immediate processing by APCs shortly after infection (9–12). Tegument proteins hence constitute an immediate target Ag for T cells (9, 10). Considering the failures during the last 2 decades of clinical herpes simplex vaccine trials using envelope glycoproteins gB and gD (21, 22), it is surprising how only a few reports of studies assessing the vaccine potential of tegument proteins exist. The present study is the first to compare the phenotype and function of HSV-1 tegument protein-specific protective CD8$^+$ T cells from HSV-seropositive SYMP and ASYMP individuals, information that is essential for the successful design of an effective T-cell-based herpes simplex vaccine. In the present study, rather than simply using a few *in vitro* predictive assays to map CD8$^+$ T-cell epitopes from HSV-1 VP13/14, we employed several computational algorithms followed by both *in vitro* and *in vivo* functional immunological assays. Only peptides that conform to given sequence motifs preferentially bind with a high affinity to HLA class I molecules (4). The amino acid residues at specific positions are conserved for peptides that bind HLA-A*02:01 molecules with a high affinity (2, 4). Potential HLA-A*02:01-binding peptides can be selected on the basis of the presence of leucine (L), isoleucine (I), or methionine (M) as the dominant residue at position 2 and valine (V) or a residue with

an aliphatic hydrocarbon side chain at the C terminus (4). Following identification of antigenic VP13/14 peptides in HLA-A*02:01-positive, HSV-1-seropositive humans, it is important to address whether each peptide can be immunogenic following correct processing from the native VP13/14 tegument protein and subsequent display on the surface of HSV-1-infected target APCs. Of the 10 antigenic VP13/14 peptides evaluated in this study, only three peptide epitopes (VP13/14$_{286-294}$, VP13/14$_{504-512}$, and VP13/14$_{544-552}$) were generated from the native VP13/14 protein by natural processing. This observation illustrates the importance of experimentally evaluating whether peptides generated by computer algorithms and various HLA-peptide binding assays are able to functionally stimulate CD8$^+$ T cells *in vitro* and *in vivo*. Many immunological assays have been developed to validate computationally predicted human CD8$^+$ T-cell epitopes, including determination of the frequency of epitope-specific CD8$^+$ T_{EM} versus T_{CM} cells by the use of tetramers; assays for cell membrane HLA stabilization; assays for CD8$^+$ T-cell cytokine production; assays for intracellular IFN-γ production; assays for the release of granules containing cytotoxic GzmB, GzmK, perforin, and CD107$^{a/b}$; and assays for detection of the PD-1 exhaustion marker (52–54). When used individually, each screen is not sufficient to conclusively identify functional CD8$^+$ T-cell epitopes (52, 54–56). Combinations of these screens, however, can comprehensively provide strong evidence of functional T-cell epitopes (15, 54, 57). Using multiple screens, we identified three high-affinity VP13/14 epitopes that were naturally processed and able to recall frequent and multifunction CD8$^+$ T_{EM} cells in HSV-1-seropositive ASYMP individuals.

The epitope-based vaccine approach has been proven to be an extremely useful strategy to avoid potentially harmful immune responses (4, 58). Among other advantages, the epitope-based vaccines avoid the potential for nonprotected epitopes to inadvertently drive unwanted responses (59). Such pathogenic responses might contribute to the exacerbation of disease, as we recently found for an HLA-A*02:01-restricted CD8$^+$ T-cell epitope from the HSV-1 gK protein (60). Moreover, focusing the immune response toward selected protective ASYMP epitopes instead of potential SYMP epitopes could be of value in the case of herpesvirus infections, where T cells directed against the SYMP epitopes might have been involved in immunopathology. The efficacy of peptide epitope-based vaccines on inducing strong and long-lived effector memory CD8$^+$ cells (T_{EM} cells) but not central memory CD8$^+$ cells (T_{CM} cells) has been reported (61). In the present study, we found an increase in the frequency of epitope-specific human CD8$^+$ T_{CM} cells following *in vitro* stimulation with SYMP peptide epitopes. In contrast, there was an increase in the frequency of epitope-specific human CD8$^+$ T_{EM} cells following *in vitro* stimulation with ASYMP peptide epitopes. Moreover, the protection induced in mice following immunization with ASYMP peptides correlated with the induction of the CD8$^+$ T_{EM}-cell phenotype *in vivo*. In contrast, the lack of protection induced in mice following immunization with SYMP epitopes correlated with the induction of the CD8$^+$ T_{CM}-cell phenotype *in vivo*. Collectively, these results from studies with both humans and mice support the symptomatic/asymptomatic concept and suggest a balance between a protective ASYMP epitope-specific T_{EM}-cell response and a nonprotective SYMP epitope-specific T_{CM}-cell response.

In addition, humans are not immunologically naive like laboratory mice that are selectively bred in sanitized environments (61). In HSV-seropositive humans, the memory CD8$^+$ T cells mature during childhood after exposure to other viruses and other pathogens, and the T-cell repertoire that develops cross-reacts with different viruses, including members of the same (or different) herpesvirus family (62–65). However, this is unlikely for the three VP13/14 epitopes identified in this study because (i) the sequences of the VP13/14$_{286-294}$, VP13/14$_{504-512}$, and VP13/14$_{544-552}$ epitopes are highly conserved between HSV-1 strains (100%) and HSV-2 strains (88%) (see Table S1 in the supplemental material); (ii) no significant homology exists between the amino acid sequences of these three epitopes and the VP13/14 amino acid sequences of varicella-zoster virus (VZV; 44% to 55%) and cytomegalovirus (CMV; 44% to 55%) strains (Table S1); (iii) the sequence alignments with published sequences of VP13/14 proteins from other human herpesviruses (e.g., VZV and CMV) did not reveal significant homol-

ogies that might be translated to functional cross-reactive T cells (Table S1); and (iv) the three HLA-A*02:01-restricted VP13/14 epitopes reported here to be recognized by $CD8^+$ T cells from HLA-A*02:01-positive, HSV-1-seropositive individuals are also recognized with the same magnitude and breadth by $CD8^+$ T cells developed in laboratory HLA-A*02:01 Tg mice that are selectively bred in sanitized environments and infected with HSV-1. These results suggest that the identified HSV-1 VP13/14 epitopes but not cross-reactive epitopes from other members of the herpesvirus family most likely contribute to the development of $CD8^+$ T cells detected from HLA-A*02:01-positive, HSV-1-seropositive individuals. However, one cannot definitely exclude the possibility of cross-reactivity of these VP13/14 epitopes with other epitopes from other pathogens outside the herpesvirus family.

We recently reported a significantly higher proportion of polyfunctional $CD8^+$ T_{EM} cells specific to HSV-1 glycoprotein gB epitopes in healthy ASYMP individuals who are seropositive for HSV-1 but never had any recurrent herpetic disease than in SYMP individuals (66). In contrast, monofunctional gB-specific $CD8^+$ T_{CM} cells are predominant in SYMP patients (66). This report extends our previous report by showing that $CD8^+$ T_{EM} cells specific to HSV-1 tegument protein VP13/14 epitopes are also present at a higher proportion in ASYMP individuals than in SYMP patients. Instead of relying on a single assay, we used several immunological assays to determine the population size, the phenotype, and the function of VP13/14 epitope-specific $CD8^+$ T cells that are predominant in the PBMCs of ASYMP individuals but not SYMP individuals. Though we are aware that information gained from PBMC-derived T cells may not be completely reflective of the information for tissue-resident T cells, our investigations were limited to human PBMC-derived $CD8^+$ T cells because of the obvious ethical and practical challenges in obtaining corneas and TG-resident $CD8^+$ T cells. Nevertheless, under these circumstances, we found that HSV-specific $CD8^+$ T cells from ASYMP patients had a greater frequency of polyfunctional $CD8^+$ T_{EM} cells specific to VP13/14 epitopes than HSV-specific $CD8^+$ T cells from SYMP patients, while $CD8^+$ T cells from SYMP individuals had more monofunctional VP13/14 epitope-specific $CD8^+$ T_{CM} cells than $CD8^+$ T cells from ASYMP individuals. These results suggest that at a second pathogen encounter (e.g., following HSV-1 reactivation from latency), ASYMP individuals would mount a faster and stronger polyfunctional HSV-specific $CD8^+$ T_{EM}-cell response than SYMP individuals and that this response would allow a fast and better clearance of herpesvirus reactivation and recurrent disease. In the present study, we found that VP13/14-specific $CD8^+$ T cells from SYMP patients expressed low levels of the transcription factors T-bet and Eomes, which are associated with a high level of PD-1. This phenotype is consistent with nondifferentiated and dysfunctional $CD8^+$ T cells in SYMP patients. In contrast, VP13/14-specific $CD8^+$ T cells from ASYMP individuals, which express no symptoms, expressed high levels of the transcription factors T-bet and Eomes, which are associated with a low level of PD-1. This phenotype is consistent with differentiated and functional $CD8^+$ T cells in ASYMP individuals. It is likely that the observed increase in the levels of T-bet and Eomes expression by $CD8^+$ T cells from ASYMP patients promotes the terminal differentiation of secondary effector and memory $CD8^+$ T_{EM} cells, as recently reported in other systems (67). On the one hand, T-bet and Eomes are key transcription factors involved in the long-term renewal of memory $CD8^+$ T cells to their characteristic effector potency (40–44). T-bet drives the differentiation of $CD8^+$ T_{EM} cells at the expense of T_{CM} cells (43). T-bet is also overexpressed in $CD8^+$ T cells that differentiated even in the absence of $CD4^+$ T-cell help, a condition that is associated with defective central memory cell (T_{CM} cell) formation (43). Eomes enables $CD8^+$ T cells to compete for the memory cell niche (41). Additionally, $CD8^+$ T cells deficient in T-bet and Eomes fail to differentiate into functional killers, which is required for defense against viral pathogens (42). Virus-specific $CD8^+$ T cells lacking both T-bet and Eomes differentiate into an interleukin-17-secreting autoimmune and inflammatory T-cell lineage (42). To our knowledge, this is the first study to show the differential expression of transcription factors in VP13/14-specific human memory $CD8^+$ T cells among HLA-A*02:01-positive, HSV-1-seropositive SYMP and ASYMP individuals. It is likely that the

concerted action of T-bet, Eomes, and other transfection factors results in the development in ASYMP individuals of fully differentiated CD8+ T_{EM} cells that migrate to inflamed tissues (i.e., eyes and sensory ganglia) following antigen recognition and secrete IFN-γ and/or release cytotoxic granules that contain GzmB and perforin (68, 69).

We detected higher levels of expression of Ki-67 in CD8+ T_{EM} cells from ASYMP individuals than in CD8+ T_{EM} cells from SYMP individuals. This result is in agreement with the findings of previous studies reporting that CD8+ T cells with the effector phenotype express more Ki-67 (70, 71). Nevertheless, the higher levels of expression of Ki-67 on T_{EM} cells and the lower levels of expression of Ki-67 on T_{CM} cells remain controversial. We also found more CD8+ T_{CM} cells with higher levels of expression of PD-1 in SYMP individuals than ASYMP individuals. This finding suggests a persistent antigenic stimulation of HSV-specific CD8+ T_{CM} cells in SYMP individuals, as recently reported in other systems (40). Exhaustion has a major role in the failure of T cells to control persistent infections, including HSV-1 infections (72, 73). The increased levels of PD-1 expression on T_{CM} cells might account for the poor effector response in SYMP individuals due to T-cell exhaustion and could be a factor contributing to the nonclearance of infection with disease progression in SYMP individuals. It should be noted that PD-1 expression by itself does not demonstrate exhaustion. However, it is well established that activated memory T cells and exhausted T cells have different levels of PD-1 expression, with exhausted CD8+ T cells expressing higher levels of PD-1 than activated memory T cells (74–76). These different levels of PD-1 can help distinguish between exhaustion and activation. Nevertheless, in the present study, the phenotypic exhaustion (dysfunction) of CD8+ T cells was confirmed at the functional level by impaired cytotoxic activity and decreased levels of IFN-γ, TNF-α, and IL-1 production.

A recent study suggests that CD8+ T cells are required to eliminate HSV-1 from the cornea but play a minimal role in immunopathology (77). Intraocular T cells derived from patients with HSV-induced acute retinal necrosis recognize VP13/14 proteins (78). The underlying protective and nonprotective mechanisms of HSV-specific CD8+ T cells in ocular herpes remain to be fully elucidated. Based on our present findings, we propose a mechanism built on the novel symptomatic/asymptomatic concept in which the corneal lesions are not a consequence of the damage caused directly by the virus or by autoreactive or bystander T cells but, rather, are the result of the balance between protective T_{EM} cells that recognize ASYMP HSV-1 epitopes and nonprotective T_{CM} cells that recognize SYMP HSV-1 epitopes within the same or different HSV-1 proteins. The polyfunctionality of CD8+ T_{EM} cells is associated with the control of herpesvirus in both ASYMP individuals and ASYMP HLA Tg mice. Thus, the polyfunctionality of HSV-specific CD8+ T_{EM} cells may be an important factor accounting for the immunologic control of herpesvirus. CD8+ T_{EM} cells from ASYMP individuals appeared to recognize naturally processed epitopes on HSV-1-infected cells and had strong virus-inhibitory cytotoxic activity. A formal demonstration that ASYMP CD8+ T_{EM} cells with these functions cause the immunologic control of recurrent herpesvirus infection and disease would require passive transfer studies in HSV-1-infected hosts that develop recurrent disease (14). Such studies are currently ongoing in our laboratory using our mouse model of UV-B-induced recurrent herpetic disease (5, 6), and the results will be the subject of future reports.

A recent human study by Pulko et al. has reported on a previously unknown subset of memory T cells with a naive CD45RA+ CCR7+ phenotype, designated T_{MNP} cells (37). These memory CD8+ T_{MNP} cells respond to persistent viruses by rapidly secreting multiple cytokines, and they differ transcriptionally from conventional memory and effector T cells (37). The opposite CD45RA+ CCR7− T cells, which express low levels of CCR7, are known as T_{EMRA} cells. We found similar frequencies of CD8+ T_{MNP} cells in SYMP and ASYMP individuals. However, more CD8+ T_{EMRA} cells appeared to be present in ASYMP individuals than SYMP individuals. An investigation of T_{EMRA} and T_{MNP} cells was outside the scope of the present study, which focused mainly on T_{EM} and T_{CM} cells. Nevertheless, we plan to investigate a potential association of CD8+ T_{MNP}- and T_{EMRA}-

cell responses with SYMP versus ASYMP herpes, and the results will be subject of a future report.

In conclusion, the present study (i) provides new insights into the phenotype and function of HSV-specific $CD8^+$ T_{EM}-cell subpopulations that are associated with the immunologic control of ocular herpesvirus infection and disease in both humans and humanized HLA-A*02:01 transgenic mice and (ii) identified three new ASYMP epitopes derived from the HSV-1 VP13/14 tegument protein that preferentially recalled the polyfunctional $CD8^+$ T_{EM}-cell responses in both HLA-A*02:01-positive, ASYMP humans and humanized HLA-A*02:01 transgenic mice that were protected from ocular herpes. Understanding the detailed mechanisms by which HSV-specific ASYMP $CD8^+$ T cells are associated with protection against ocular herpes is critical for the rational design of a T-cell-based herpes simplex vaccine.

MATERIALS AND METHODS

Human study population. During the last decade (i.e., January 2003 to August 2016), we have screened 781 individuals for HSV-1 and HSV-2 seropositivity (Table 2). Of these individuals, 543 individuals were white, 238 were nonwhite (African, Asian, Hispanic, or other), 395 were female, and 386 were male. Among these individuals, a cohort of 283 immunocompetent individuals with an age range of 21 to 67 years (median age, 30 years) who were seropositive for HSV-1 and seronegative for HSV-2 were enrolled in the present study. All enrolled patients were negative for HIV and hepatitis B virus and had no history of immunodeficiency. Six hundred eighty patients were HSV-1, HSV-2, or HSV-1 and HSV-2 seropositive, 711 patients were healthy and ASYMP (ASYMP individuals were individuals who, in the absence of therapy, had never had any recurrent herpes disease at an ocular, genital, or any other location, on the basis of their self-report and physician examination; a single episode of any herpetic disease [at any point in life] would exclude the individual from this group). The remaining 70 patients were defined to be HSV-seropositive SYMP individuals with frequent and severe recurrent genital, ocular, and/or orofacial lesions, with two patients having had clinically well-documented repetitive herpes stromal keratitis (HSK) (one patient had had ~20 episodes over 20 years that necessitated several corneal transplantations).

Signs of recurrent disease in SYMP patients were defined as herpetic lid lesions, herpetic conjunctivitis, dendritic or geographic keratitis, stromal keratitis, and iritis consistent with HSK at a frequency of one or more episodes per year for the past 2 years. At the time of blood sample collection, however, SYMP patients had no recurrent disease (other than corneal scarring) and had had no recurrences during the previous 30 days. SYMP patients had no ocular disease other than HSK, had no history of recurrent genital herpes, and were HSV-1 seropositive and HSV-2 seronegative. Due to the wide spectrum of recurrent ocular herpetic disease, our emphasis was primarily on the number of recurrent episodes rather than the severity of the recurrent disease. Therefore, no attempt was made to assign specific T-cell epitopes to a specific severity of recurrent lesions. Patients were also excluded if they (i) were pregnant or breastfeeding or (ii) were on acyclovir, other related antiviral drugs, or any immunosuppressive drugs at the time of blood sample collection. The SYMP and ASYMP groups were matched for age, gender, serological status, and race. Eighty-six healthy control individuals were seronegative for both HSV-1 and HSV-2 and had no history of ocular herpes, genital lesions, or orofacial herpes disease. All subjects were enrolled at the University of California, Irvine, under Institutional Review Board (IRB)-approved protocols (IRB number 2003-3111 and IRB number 2009-6963). Written informed consent was received from all participants prior to inclusion in the study.

Bioinformatics analyses. The HSV-1 VP13/14 open reading frames utilized in this study were from strain 17 (UniProt accession number P10231). The 693-amino-acid sequence of the VP13/14 protein (see Fig. S1 in the supplemental material) was screened for HLA-A2.1-restricted epitopes using different computational algorithms, as previously described: BIMAS software (Bioinformatics and Molecular Analysis Section, NIH, Bethesda, MD), the SYFPEITHI algorithm (http://www.syfpeithi.de/), and the MAPPP algorithm (http://www.mpiib-berlin.mpg.de/MAPPP) (4, 15). Potential cleavage sites for human proteasome were also employed in this screening and were identified using NetChop (version 3.0) software (http://www.cbs.dtu.dk/services/NetChop/) (4, 15).

Peptide synthesis. To determine potential vaccine candidates, 10 HLA-A*02:01-binding peptides of herpes simplex virus 1 (strain 17) VP13/14 with a long estimated half-life of dissociation ($t_{1/2}$) were synthesized by Magenex (San Diego, CA) on a 9050 Pep synthesizer instrument using solid-phase peptide synthesis and standard 9-fluorenylmethoxy carbonyl technology (PE Applied Biosystems, Foster City, CA). Stock solutions were made at 1 mg/ml in phosphate-buffered saline (PBS). All peptides were stored in aliquots at −20°C until assayed.

Cell lines. Cells of the T2 mutant hybrid cell line (174 cells × CEM.T2 cells) derived from the T-lymphoblast cell line CEM were obtained from ATCC. T_2 cells lack the functional transporter associated with antigen processing (TAP) heterodimer and fail to express normal amounts of HLA-A*02:01 on the cell surface. HLA-A*02:01 surface expression can be stabilized with exogenous loading of peptides that are able to bind to the MHC class I molecule. The T_2 cell line was maintained in Iscove modified Dulbecco medium (ATCC) supplemented with 10% heat-inactivated fetal bovine serum (FBS), 100 U of penicillin/ml, and 100 U of streptomycin/ml (Sigma-Aldrich, St. Louis, MO).

Stabilization of HLA-A*02:01 on class I HLA-transfected B × T hybrid cells. To determine whether synthetic peptides could stabilize HLA-A*02:01 molecule expression on the T2 cell surface, peptide-inducing HLA-A*02:01 upregulation on T2 cells was examined according to a previously described protocol (79, 80). T2 cells (3×10^5/well) were incubated with different concentrations of the individual VP13/14 peptides (Fig. 1) in 48-well plates for 18 h at 26°C. The cells were then incubated at 37°C for 3 h in the presence of 0.7 μl/ml BD GolgiStop protein transport inhibitor to block the cell surface expression of newly synthesized HLA-A*02:01 molecules and human β_2-microglobulin (1 μg/ml). The cells were washed with FACS buffer (1% bovine serum albumin and 0.1% sodium azide in phosphate-buffered saline) and stained with anti-HLA-A2.1-specific monoclonal antibody (clone BB7.2; BD-Pharmingen, USA) at 4°C for 30 min. After incubation, the cells were washed with FACS buffer, fixed with 1% paraformaldehyde in phosphate-buffered saline, and analyzed by flow cytometry using an LSRII flow cytometer (Becton, Dickinson). The acquired data were analyzed with FlowJo software (BD Biosciences, San Jose, CA). Expression was measured by use of the LSRII flow cytometer, and the mean fluorescence intensity (MFI) was recorded. The percent increase in the MFI was calculated as follows: percent increase in the MFI = [(MFI with the given peptide − MFI without peptide)/(MFI without peptide)] × 100. Each experiment was performed 3 times, and means ± standard deviations (SDs) were calculated.

HSV-specific serotyping by ELISA. The serum samples collected from random donors were tested for anti-HSV antibodies. An enzyme-linked immunosorbent assay (ELISA) was performed in sterile 96-well flat-bottomed microplates. The plates were coated with the HSV-1 antigen in coating buffer overnight at 4°C. On the next day, the plates were washed with PBS–1% Tween 20 (PBST) five times. Nonspecific binding was blocked by incubation with a 5% solution of skimmed milk in PBS (200 μl/well) at 4°C for 1 h at room temperature. The microplates were washed three times with PBS–Tween 20 and incubated with various serum samples at 37°C for 2 h. Following five washes, biotinylated rabbit anti-human IgG, diluted 1:20,000 with PBST, was used as the secondary antibody, and the mixture was incubated at 37°C for 2 h. After five washes, streptavidin was added at a 1:5,000 dilution and the mixture was incubated for 30 min at room temperature. After five additional washes, the color was developed by adding 100 μl of tetramethylbenzidine substrate. The mixture was incubated for 5 to 15 min at room temperature in the absence of light. The reaction was terminated by adding 1 M H_2SO_4. The absorbance was measured at 450 nm.

PBMC isolation. One hundred milliliters of an individual's blood was drawn into yellow-top Vacutainer tubes (Becton, Dickinson, USA). The peripheral blood mononuclear cells (PBMCs) were isolated by gradient centrifugation using leukocyte separation medium (Cellgro, USA). The cells were washed in PBS and resuspended in complete culture medium consisting of RPMI 1640 medium containing 10% fetal bovine serum (FBS; Bio-Products, Woodland, CA, USA) supplemented with 1× penicillin, L-glutamine, streptomycin, 1× sodium pyruvate, 1× nonessential amino acids, and 50 μM 2-mercaptoethanol (Life Technologies, Rockville, MD, USA). Aliquots of freshly isolated PBMCs were also cryopreserved in 90% FBS and 10% dimethyl sulfoxide in liquid nitrogen for future testing.

HLA-A2 typing. The HLA-A2 status was confirmed by staining of PBMCs with 2 μl of anti-HLA-A2 MAb (clone BB7.2; BD-Pharmingen, USA) at 4°C for 30 min. The cells were washed and analyzed by flow cytometry using an LSRII flow cytometer (Becton, Dickinson). The acquired data were analyzed with FlowJo software (BD Biosciences, San Jose, CA).

Flow cytometry analysis. PBMCs were analyzed by flow cytometry after staining with fluorochrome-conjugated human-specific MAbs. The antihuman antibodies were CD3 (clone SK7) conjugated to phycoerythrin (PE)-Cy7, CD44 (clone G44-26) conjugated to A700, CD8 (clone SK1) conjugated to allophycocyanin (APC)-Cy7, CCR7 (clone 150503) conjugated to Alexa Fluor 700, CD45RA conjugated to fluorescein isothiocyanate (FITC), CD62L conjugated to APC, IFN-γ conjugated to Alexa Fluor 647, T-bet (clone O4-46) conjugated to Alexa Fluor 488 (BD Pharmingen), granzyme B (clone GB11) conjugated to A647, CD107^a (clone H4A3) conjugated to FITC, CD107^b (clone H4B4) conjugated to FITC (BioLegend), granzyme K (clone G3H69) conjugated to peridinin chlorophyll protein-eFlour 710, perforin (clone d69) conjugated to FITC, and Eomes (clone WD1928) conjugated to eFluor 660 (eBioscience). Corneal cells were analyzed by flow cytometry after staining with fluorochrome-conjugated mouse-specific MAbs. The antimouse antibodies were CD8 (clone 53-6.7) conjugated to PE-Cy7, CD44 (clone IM7) conjugated to APC-Cy7, CD62L (MEL-14) conjugated to A700, CD107a (clone 1D4B) conjugated to FITC, CD107b (clone Ha1/29) conjugated to FITC, and IFN-γ (clone XMG1.2) conjugated to A700 (BD Pharmingen).

Surface-staining MAbs against various cell markers were added to a total of 1×10^6 PBMCs in PBS containing 1% FBS and 0.1% sodium azide (FACS buffer) for 45 min at 4°C. After the cells were washed with FACS buffer, they were permeabilized for 20 min on ice using a Cytofix/Cytoperm kit (BD Biosciences) and then washed twice with Perm/Wash buffer (BD Bioscience). Intracellular cytokine-staining MAbs were then added to the cells, and the mixture was incubated for 45 min on ice in the dark. The cells were washed again with Perm/Wash buffer and FACS buffer and fixed in PBS containing 2% paraformaldehyde (Sigma-Aldrich, St. Louis, MO). Two hundred thousand total events were acquired for each sample on a BD LSRII Fortessa flow cytometer. Antibody capture beads (BD Biosciences) were used as individual compensation tubes for each fluorophore in the experiment. We defined positive and negative populations by employing the fluorescence minus the fluorescence for the controls for each fluorophore used in this study when initially developing the staining protocols. In addition, we further optimized gating by examining known negative cell populations for the background level of expression. The gating strategy was similar to that used in our previous work (15). We briefly gated on single cells, dump-negative cells, viable cells (Aqua Blue), lymphocytes, CD3$^+$ cells, and CD8$^+$ cells before the final gating on functional cells. For epitope-specific cells, VP13/14 tetramer-specific CD8$^+$ T cells were gated

for the different markers used for costaining. Data analysis was performed using FlowJo (version 9.7.5) software (TreeStar, Ashland, OR). Statistical analyses were done using GraphPad Prism (version 5) software (La Jolla, CA).

mRNA isolation and real-time RT-PCR analysis. Total RNA was isolated from fresh PBMCs using a Direct-zol RNA miniprep kit (Zymo Research) and reverse transcribed with a high-capacity cDNA reverse transcription kit (Applied Biosystems) according to the manufacturer's instructions. Quantitative real-time PCR was carried out on a Rotor-Gene 3000 PCR cycler (Corbett Research) using LightCycler 480 SYBR green 1 master mix (Roche). The data were normalized to those for GAPDH (glyceraldehyde-3-phosphate dehydrogenase) for transcription factor analysis. Relative mRNA expression levels were calculated using the following formula: ratio = $(E_{target}^{\Delta CP_{target}}(\text{control} - \text{sample})/(E_{ref}^{\Delta CP_{ref}}(\text{control} - \text{sample})$, where E_{target} is the efficiency of the target gene, ΔCP_{target} is the normalized cycle threshold of the target gene, E_{ref} is the efficiency of the reference gene, ΔCP_{ref} is the normalized cycle threshold of the reference gene, and control − sample indicates the level of mRNA expression for the GAPDH control minus the level of expression of mRNA for the sample. The data are expressed as the fold increase.

Tetramer–VP13/14 peptide staining. Fresh PBMCs were analyzed for the frequency of $CD8^+$ T cells recognizing the VP13/14 peptide–tetramer complexes, as we previously described (9–12). The cells were incubated with the VP13/14 peptide–tetramer complex for 30 to 45 min at 37°C. The cell preparations were then washed with FACS buffer and stained with FITC-conjugated anti-human CD8 MAb (BD Pharmingen). The cells were washed and fixed with 1% paraformaldehyde in PBS. The cells were then acquired on a BD LSRII flow cytometer, and the data were analyzed using FlowJo (version 9.5.6) software (TreeStar).

CD107 cytotoxicity assay. To detect VP13/14-specific cytolytic $CD8^+$ T cells in PBMCs and corneal cells, an intracellular $CD107^{a/b}$ cytotoxicity assay was performed as described by Betts and colleagues with a few modifications (38, 81). PBMCs (1×10^6) from patients, in addition to spleen cells from mice infected with HSV, were transferred into 96-well V-bottom FACS plates (BD) in R10 medium (RPMI 1640 medium containing 10% fetal bovine serum; Cellgro) and stimulated with 10 different VP13/14 peptides (10 μg/ml) in the presence of anti-$CD107^a$-FITC and $CD107^b$-FITC (BD Pharmingen) and BD GolgiStop protein transport inhibitor (10 μg/ml) for 5 to 6 h at 37°C. Cells receiving concanavalin A (10 μg/ml; Sigma-Aldrich) and no peptide were used as positive and negative controls, respectively. At the end of the incubation period, the cells were harvested into separate tubes, washed once with FACS buffer, and then stained with PE-conjugated anti-human CD8 antibody for 30 min. The cells were fixed, permeabilized, and stained with additional antibodies against IFN-γ using a Cytofix/Cytoperm kit and Perm/Wash solution (BD).

Cytokine assay. Fresh PBMCs (5×10^5 cells) were stimulated in a 96-well plate with or without individual peptides bearing potential $CD8^+$ T-cell epitopes from VP13/14 for 96 h. Supernatants were collected, and the production of the IFN-γ, TNF-α, and IL-2 cytokines was assayed using multiplex cytokine arrays (Millipore) per the manufacturer's protocols. Samples were acquired on a Magpix system (Luminex).

HLA-A*02:01 transgenic mice. HLA-A*02:01 transgenic mice, which have been described previously (29, 30, 82), were kindly provided by Francois Lemonier (Pasteur Institute, Paris, France) and were bred at the University of California, Irvine. All animal studies were conducted in facilities approved by the Association for Assessment and Accreditation of Laboratory Animal Care and according to Institutional Animal Care and Use Committee-approved animal protocols (IACUC number 2002-2372).

Virus production. HSV-1 (strain McKrae) was grown and titrated on rabbit skin (RS) cells. UV-inactivated HSV-1 was generated as we previously described (13). HSV inactivation was confirmed by the inability to produce plaques when tested on RS cells.

Ocular challenge of humanized HLA transgenic mice with HSV-1. Two groups of age-matched female HLA-A*02:01 transgenic mice were challenged with 2×10^5 PFU of strain McKrae via eye drops. Control mice were inoculated using samples mock infected with virus. Following ocular challenge, the mice were monitored for ocular herpesvirus infection and disease. Some mice remained asymptomatic (they exhibited no symptoms or disease), whereas others developed symptoms and were considered symptomatic.

Immunization of mice with SYMP and ASYMP VP13/14 epitopes. Age-matched female HLA-A*02:01 transgenic mice ($n = 10$ each) were immunized subcutaneously on days 0 and day 21 with the ASYMP $CD8^+$ T-cell human epitopes selected from the HSV-1 VP13/14 tegument protein ($VP13/14_{286-294}$, $VP13/14_{504-512}$, and $VP13/14_{544-552}$) or SYMP $CD8^+$ T-cell human epitopes ($VP13/14_{410-418}$, $VP13/14_{497-505}$, and $VP13/14_{657-665}$), delivered in mixtures with the $CD4^+$ T-cell PADRE epitope and emulsified in CpG_{1826} adjuvant. All immunizations were carried out with 100 μM each peptide. Control mice received CpG_{1826} adjuvant alone (mock immunization) on days 0 and day 21. At 2 weeks after the final immunization, the mice received an ocular HSV-1 challenge with 2×10^5 PFU (strain McKrae).

Monitoring of ocular herpesvirus infection and disease. Ocular disease and virus titration were assessed immediately before inoculation and on days 1, 3, 5, 7, 10, 14, and 21 postinfection (p.i.). Animals were examined for signs of ocular disease by investigators blind to the treatment regimen, as we previously described (35). Eye swab samples were taken, and HSV-1 was titrated on RS cell monolayers (35). Mice were also examined for survival over a window of 30 days after challenge (35).

Statistical analyses. Data for each assay were compared by analysis of variance (ANOVA) and Student's unpaired *t* test using GraphPad Prism (version 5) software (La Jolla, CA). Differences between the groups were identified by ANOVA and multiple-comparison procedures, as we previously described (83). Data are expressed as the mean ± SD. Results were considered statistically significant when the *P* value was <0.05.

SUPPLEMENTAL MATERIAL

Supplemental material for this article may be found at https://doi.org/10.1128/JVI.01793-16.

TEXT S1, PDF file, 0.1 MB.

ACKNOWLEDGMENTS

This work is supported by Public Health Service research grants EY026103, EY019896, and EY024618 from the National Eye Institute (NEI) and AI110902 from the National Institute of Allergy and Infectious Diseases (NIAID), by the Discovery Center for Eye Research (DCER), and by a Research to Prevent Blindness (RPB) grant.

We declare that no conflict of interest exists.

We thank Dale Long from the NIH Tetramer Facility (Emory University, Atlanta, GA) for providing the tetramers used in this study. We also thank Barbara Bodenhoefer from the University of California, Irvine, Institute for Clinical and Translational Science (ICTS) for helping with the collection of blood from HSV-1-seropositive symptomatic and asymptomatic individuals.

REFERENCES

1. Srivastava R, Khan AA, Spencer D, Vahed H, Lopes PP, Thai NT, Wang C, Pham TT, Huang J, Scarfone VM, Nesburn AB, Wechsler SL, BenMohamed L. 2015. HLA-A02:01-restricted epitopes identified from the herpes simplex virus tegument protein VP11/12 preferentially recall polyfunctional effector memory CD8+ T cells from seropositive asymptomatic individuals and protect humanized HLA-A*02:01 transgenic mice against ocular herpes. J Immunol 194:2232–2248. https://doi.org/10.4049/jimmunol.1402606.
2. Samandary S, Kridane-Miledi H, Sandoval JS, Choudhury Z, Langa-Vives F, Spencer D, Chentoufi AA, Lemonnier FA, BenMohamed L. 2014. Associations of HLA-A, HLA-B and HLA-C alleles frequency with prevalence of herpes simplex virus infections and diseases across global populations: implication for the development of an universal CD8+ T-cell epitope-based vaccine. Hum Immunol 75:715–729. https://doi.org/10.1016/j.humimm.2014.04.016.
3. Looker KJ, Magaret AS, May MT, Turner KM, Vickerman P, Gottlieb SL, Newman LM. 2015. Global and regional estimates of prevalent and incident herpes simplex virus type 1 infections in 2012. PLoS One 10:e0140765. https://doi.org/10.1371/journal.pone.0140765.
4. Dervillez X, Qureshi H, Chentoufi AA, Khan AA, Kritzer E, Yu DC, Diaz OR, Gottimukkala C, Kalantari M, Villacres MC, Scarfone VM, McKinney DM, Sidney J, Sette A, Nesburn AB, Wechsler SL, BenMohamed L. 2013. Asymptomatic HLA-A*02:01-restricted epitopes from herpes simplex virus glycoprotein B preferentially recall polyfunctional CD8+ T cells from seropositive asymptomatic individuals and protect HLA transgenic mice against ocular herpes. J Immunol 191:5124–5138. https://doi.org/10.4049/jimmunol.1301415.
5. BenMohamed L, Osorio N, Srivastava R, Khan AA, Simpson JL, Wechsler SL. 2015. Decreased reactivation of a herpes simplex virus type 1 (HSV-1) latency-associated transcript (LAT) mutant using the in vivo mouse UV-B model of induced reactivation. J Neurovirol 21:508–517. https://doi.org/10.1007/s13365-015-0348-9.
6. BenMohamed L, Osorio N, Khan AA, Srivastava R, Huang L, Krochma JJ, Garcia LM, Simpson JL, Wechsler SL. 2016. Prior corneal scarification and injection of immune serum are not required before ocular HSV-1 infection for UV-B induced virus reactivation and recurrent herpetic corneal disease in latently infected mice. Curr Eye Res 41:747–756. https://doi.org/10.3109/02713683.2015.1061024.
7. Khan AA, Srivastava R, Chentoufi AA, Geertsema R, Thai NT, Dasgupta G, Osorio N, Kalantari M, Nesburn AB, Wechsler SL, BenMohamed L. 2015. Therapeutic immunization with a mixture of herpes simplex virus 1 glycoprotein D-derived asymptomatic human CD8+ T-cell epitopes decreases spontaneous ocular shedding in latently infected HLA transgenic rabbits: association with low frequency of local PD-1+ TIM-3+ CD8+ exhausted T cells. J Virol 89:6619–6632. https://doi.org/10.1128/JVI.00788-15.
8. Farooq AV, Shukla D. 2012. Herpes simplex epithelial and stromal keratitis: an epidemiologic update. Surv Ophthalmol 57:448–462. https://doi.org/10.1016/j.survophthal.2012.01.005.
9. Long D, Skoberne M, Gierahn TM, Larson S, Price JA, Clemens V, Baccari AE, Cohane KP, Garvie D, Siber GR, Flechtner JB. 2014. Identification of novel virus-specific antigens by CD4(+) and CD8(+) T cells from asymptomatic HSV-2 seropositive and seronegative donors. Virology 464-465:296–311. https://doi.org/10.1016/j.virol.2014.07.018.
10. Hosken N, McGowan P, Meier A, Koelle DM, Sleath P, Wagener F, Elliott M, Grabstein K, Posavad C, Corey L. 2006. Diversity of the CD8+ T-cell response to herpes simplex virus type 2 proteins among persons with genital herpes. J Virol 80:5509–5515. https://doi.org/10.1128/JVI.02659-05.
11. Dasgupta G, Chentoufi AA, Kalantari M, Falatoonzadeh P, Chun S, Lim CH, Felgner PL, Davies DH, BenMohamed L. 2012. Immunodominant asymptomatic herpes simplex virus 1 and 2 protein antigens identified by probing whole-ORFome microarrays with serum antibodies from seropositive asymptomatic versus symptomatic individuals. J Virol 86:4358–4369. https://doi.org/10.1128/JVI.07107-11.
12. Kalantari-Dehaghi M, Chun S, Chentoufi AA, Pablo J, Liang L, Dasgupta G, Molina DM, Jasinskas A, Nakajima-Sasaki R, Felgner J, Hermanson G, BenMohamed L, Felgner PL, Davies DH. 2012. Discovery of potential diagnostic and vaccine antigens in herpes simplex virus 1 and 2 by proteome-wide antibody profiling. J Virol 86:4328–4339. https://doi.org/10.1128/JVI.05194-11.
13. Zhang X, Dervillez X, Chentoufi AA, Badakhshan T, Bettahi I, Benmohamed L. 2012. Targeting the genital tract mucosa with a lipopeptide/recombinant adenovirus prime/boost vaccine induces potent and long-lasting CD8+ T cell immunity against herpes: importance of MyD88. J Immunol 189:4496–4509. https://doi.org/10.4049/jimmunol.1201121.
14. Chentoufi AA, Dasgupta G, Christensen ND, Hu J, Choudhury ZS, Azeem A, Jester JV, Nesburn AB, Wechsler SL, BenMohamed L. 2010. A novel HLA (HLA-A*0201) transgenic rabbit model for preclinical evaluation of human CD8+ T cell epitope-based vaccines against ocular herpes. J Immunol 184:2561–2571. https://doi.org/10.4049/jimmunol.0902322.
15. Chentoufi AA, Zhang X, Lamberth K, Dasgupta G, Bettahi I, Nguyen A, Wu M, Zhu X, Mohebbi A, Buus S, Wechsler SL, Nesburn AB, BenMohamed L. 2008. HLA-A*0201-restricted CD8+ cytotoxic T lymphocyte epitopes identified from herpes simplex virus glycoprotein D. J Immunol 180:426–437. https://doi.org/10.4049/jimmunol.180.1.426.
16. Langenberg AG, Corey L, Ashley RL, Leong WP, Straus SE. 1999. A prospective study of new infections with herpes simplex virus type 1 and type 2. Chiron HSV Vaccine Study Group. N Engl J Med 341:1432–1438.
17. Dasgupta G, BenMohamed L. 2011. Of mice and not humans: how reliable are animal models for evaluation of herpes CD8(+)-T cell-epitopes-based immunotherapeutic vaccine candidates? Vaccine 29:5824–5836. https://doi.org/10.1016/j.vaccine.2011.06.083.
18. Chentoufi AA, Binder NR, Berka N, Durand G, Nguyen A, Bettahi I, Maillere B, BenMohamed L. 2008. Asymptomatic human CD4+ cytotoxic T-cell epitopes identified from herpes simplex virus glycoprotein B. J Virol 82:11792–11802. https://doi.org/10.1128/JVI.00692-08.
19. Zhang X, Issagholian A, Berg EA, Fishman JB, Nesburn AB, BenMohamed L. 2005. Th-cytotoxic T-lymphocyte chimeric epitopes extended by

Nepsilon-palmitoyl lysines induce herpes simplex virus type 1-specific effector CD8+ Tc1 responses and protect against ocular infection. J Virol 79:15289–15301. https://doi.org/10.1128/JVI.79.24.15289-15301.2005.
20. Kuo T, Wang C, Badakhshan T, Chilukuri S, BenMohamed L. 2014. The challenges and opportunities for the development of a T-cell epitope-based herpes simplex vaccine. Vaccine 34:715–729. https://doi.org/10.1016/j.vaccine.2014.10.002.
21. Stanberry LR, Spruance SL, Cunningham AL, Bernstein DI, Mindel A, Sacks S, Tyring S, Aoki FY, Slaoui M, Denis M, Vandepapeliere P, Dubin G. 2002. Glycoprotein-D-adjuvant vaccine to prevent genital herpes. N Engl J Med 347:1652–1661. https://doi.org/10.1056/NEJMoa011915.
22. Belshe PB, Leone PA, Bernstein DI, Wald A, Levin MJ, Stapleton JT, Gorfinkel I, Morrow RLA, Ewell MG, Stokes-Riner A, Dubin G, Heineman TC, Schulte JM, Deal CD. 2012. Efficacy results of a trial of a herpes simplex vaccine. N Engl J Med 366:34–43. https://doi.org/10.1056/NEJMoa1103151.
23. Banerjee K, Biswas PS, Rouse BT. 2005. Elucidating the protective and pathologic T cell species in the virus-induced corneal immunoinflammatory condition herpetic stromal keratitis. J Leukoc Biol 77:24–32.
24. Stuart PM, Summers B, Morris JE, Morrison LA, Leib DA. 2004. CD8(+) T cells control corneal disease following ocular infection with herpes simplex virus type 1. J Gen Virol 85:2055–2063. https://doi.org/10.1099/vir.0.80049-0.
25. Banerjee K, Deshpande S, Zheng M, Kumaraguru U, Schoenberger SP, Rouse BT. 2002. Herpetic stromal keratitis in the absence of viral antigen recognition. Cell Immunol 219:108–118. https://doi.org/10.1016/S0008-8749(02)00601-9.
26. Bouley DM, Kanangat S, Wire W, Rouse BT. 1995. Characterization of herpes simplex virus type-1 infection and herpetic stromal keratitis development in IFN-gamma knockout mice. J Immunol 155:3964–3971.
27. Babu JS, Thomas J, Kanangat S, Morrison LA, Knipe DM, Rouse BT. 1996. Viral replication is required for induction of ocular immunopathology by herpes simplex virus. J Virol 70:101–107.
28. Koelle DM, Chen HB, Gavin MA, Wald A, Kwok WW, Corey L. 2001. CD8 CTL from genital herpes simplex lesions: recognition of viral tegument and immediate early proteins and lysis of infected cutaneous cells. J Immunol 166:4049–4058. https://doi.org/10.4049/jimmunol.166.6.4049.
29. Boucherma R, Kridane-Miledi H, Bouziat R, Rasmussen M, Gatard T, Langa-Vives F, Lemercier B, Lim A, Berard M, Benmohamed L, Buus S, Rooke R, Lemonnier FA. 2013. HLA-A*01:03, HLA-A*24:02, HLA-B*08:01, HLA-B*27:05, HLA-B*35:01, HLA-B*44:02, and HLA-C*07:01 monochain transgenic/H-2 class I null mice: novel versatile preclinical models of human T cell responses. J Immunol 191:583–593. https://doi.org/10.4049/jimmunol.1300483.
30. BenMohamed L, Krishnan R, Longmate J, Auge C, Low L, Primus J, Diamond DJ. 2000. Induction of CTL response by a minimal epitope vaccine in HLA A*0201/DR1 transgenic mice: dependence on HLA class II restricted T(H) response. Hum Immunol 61:764–779. https://doi.org/10.1016/S0198-8859(00)00139-7.
31. Benmohamed L, Thomas A, Bossus M, Brahimi K, Wubben J, Gras-Masse H, Druilhe P. 2000. High immunogenicity in chimpanzees of peptides and lipopeptides derived from four new Plasmodium falciparum pre-erythrocytic molecules. Vaccine 18:2843–2855. https://doi.org/10.1016/S0264-410X(00)00068-2.
32. Daubersies P, Thomas AW, Millet P, Brahimi K, Langermans JA, Ollomo B, BenMohamed L, Slierendregt B, Eling W, Van Belkum A, Dubreuil G, Meis JF, Guerin-Marchand C, Cayphas S, Cohen J, Gras-Masse H, Druilhe P. 2000. Protection against Plasmodium falciparum malaria in chimpanzees by immunization with the conserved pre-erythrocytic liver-stage antigen 3. Nat Med 6:1258–1263. https://doi.org/10.1038/81366.
33. Bottius E, BenMohamed L, Brahimi K, Gras H, Lepers JP, Raharimalala L, Aikawa M, Meis J, Slierendregt B, Tartar A, Thomas A, Druilhe P. 1996. A novel Plasmodium falciparum sporozoite and liver stage antigen (SALSA) defines major B, T helper, and CTL epitopes. J Immunol 156:2874–2884.
34. McKinney DM, Skvoretz R, Livingston BD, Wilson CC, Anders M, Chesnut RW, Sette A, Essex M, Novitsky V, Newman MJ. 2004. Recognition of variant HIV-1 epitopes from diverse viral subtypes by vaccine-induced CTL. J Immunol 173:1941–1950. https://doi.org/10.4049/jimmunol.173.3.1941.
35. Kessler JH, Beekman NJ, Bres-Vloemans SA, Verdijk P, van Veelen PA, Kloosterman-Joosten AM, Vissers DC, ten Bosch GJ, Kester MG, Sijts A, Wouter Drijfhout J, Ossendorp F, Offringa R, Melief CJ. 2001. Efficient identification of novel HLA-A(*)0201-presented cytotoxic T lymphocyte epitopes in the widely expressed tumor antigen PRAME by proteasome-mediated digestion analysis. J Exp Med 193:73–88. https://doi.org/10.1084/jem.193.1.73.
36. Sallusto F, Lenig D, Forster R, Lipp M, Lanzavecchia A. 1999. Two subsets of memory T lymphocytes with distinct homing potentials and effector functions. Nature 401:708–712. https://doi.org/10.1038/44385.
37. Pulko V, Davies JS, Martinez C, Lanteri MC, Busch MP, Diamond MS, Knox K, Bush EC, Sims PA, Sinari S, Billheimer D, Haddad EK, Murray KO, Wertheimer AM, Nikolich-Zugich J. 2016. Human memory T cells with a naive phenotype accumulate with aging and respond to persistent viruses. Nat Immunol 17:966–975. https://doi.org/10.1038/ni.3483.
38. Betts MR, Brenchley JM, Price DA, De Rosa SC, Douek DC, Roederer M, Koup RA. 2003. Sensitive and viable identification of antigen-specific CD8+ T cells by a flow cytometric assay for degranulation. J Immunol Methods 281:65–78. https://doi.org/10.1016/S0022-1759(03)00265-5.
39. Channappanavar R, Twardy BS, Suvas S. 2012. Blocking of PDL-1 interaction enhances primary and secondary CD8 T cell response to herpes simplex virus-1 infection. PLoS One 7:e39757. https://doi.org/10.1371/journal.pone.0039757.
40. Kao C, Oestreich KJ, Paley MA, Crawford A, Angelosanto JM, Ali MA, Intlekofer AM, Boss JM, Reiner SL, Weinmann AS, Wherry EJ. 2011. Transcription factor T-bet represses expression of the inhibitory receptor PD-1 and sustains virus-specific CD8+ T cell responses during chronic infection. Nat Immunol 12:663–671. https://doi.org/10.1038/ni.2046.
41. Banerjee A, Gordon SM, Intlekofer AM, Paley MA, Mooney EC, Lindsten T, Wherry EJ, Reiner SL. 2010. Cutting edge: the transcription factor eomesodermin enables CD8+ T cells to compete for the memory cell niche. J Immunol 185:4988–4992. https://doi.org/10.4049/jimmunol.1002042.
42. Intlekofer AM, Banerjee A, Takemoto N, Gordon SM, Dejong CS, Shin H, Hunter CA, Wherry EJ, Lindsten T, Reiner SL. 2008. Anomalous type 17 response to viral infection by CD8+ T cells lacking T-bet and eomesodermin. Science 321:408–411. https://doi.org/10.1126/science.1159806.
43. Intlekofer AM, Takemoto N, Kao C, Banerjee A, Schambach F, Northrop JK, Shen H, Wherry EJ, Reiner SL. 2007. Requirement for T-bet in the aberrant differentiation of unhelped memory CD8+ T cells. J Exp Med 204:2015–2021. https://doi.org/10.1084/jem.20070841.
44. Takemoto N, Intlekofer AM, Northrup JT, Wherry EJ, Reiner SL. 2006. Cutting edge: IL-12 inversely regulates T-bet and eomesodermin expression during pathogen-induced CD8+ T cell differentiation. J Immunol 177:7515–7519. https://doi.org/10.4049/jimmunol.177.11.7515.
45. Joshi NS, Kaech SM. 2008. Effector CD8 T cell development: a balancing act between memory cell potential and terminal differentiation. J Immunol 180:1309–1315. https://doi.org/10.4049/jimmunol.180.3.1309.
46. Bernardin F, Kong D, Peddada L, Baxter-Lowe LA, Delwart E. 2005. Human immunodeficiency virus mutations during the first month of infection are preferentially found in known cytotoxic T-lymphocyte epitopes. J Virol 79:11523–11528. https://doi.org/10.1128/JVI.79.17.11523-11528.2005.
47. Wang QJ, Huang XL, Rappocciolo G, Jenkins FJ, Hildebrand WH, Fan Z, Thomas EK, Rinaldo CR, Jr. 2002. Identification of an HLA A*0201-restricted CD8(+) T-cell epitope for the glycoprotein B homolog of human herpesvirus 8. Blood 99:3360–3366. https://doi.org/10.1182/blood.V99.9.3360.
48. Pelte C, Cherepnev G, Wang Y, Schoenemann C, Volk HD, Kern F. 2004. Random screening of proteins for HLA-A*0201-binding nine-amino acid peptides is not sufficient for identifying CD8 T cell epitopes recognized in the context of HLA-A*0201. J Immunol 172:6783–6789. https://doi.org/10.4049/jimmunol.172.11.6783.
49. Stock AT, Jones CM, Heath WR, Carbone FR. 2006. CTL response compensation for the loss of an immunodominant class I-restricted HSV-1 determinant. Immunol Cell Biol 84:543–550. https://doi.org/10.1111/j.1440-1711.2006.01469.x.
50. Storkus WJ, Zarour HM. 2000. Melanoma antigens recognised by CD8+ and CD4+ T cells. Forum (Genova) 10:256–270.
51. Wallace ME, Keating R, Heath WR, Carbone FR. 1999. The cytotoxic T-cell response to herpes simplex virus type 1 infection of C57BL/6 mice is almost entirely directed against a single immunodominant determinant. J Virol 73:7619–7626.
52. Hertz T, Yanover C. 2007. Identifying HLA supertypes by learning distance functions. Bioinformatics 23:e148–e155. https://doi.org/10.1093/Bioinformatics/btl324.
53. Botten J, Alexander J, Pasquetto V, Sidney J, Barrowman P, Ting J, Peters B, Southwood S, Stewart B, Rodriguez-Carreno MP, Mothe B, Whitton JL,

Sette A, Buchmeier MJ. 2006. Identification of protective Lassa virus epitopes that are restricted by HLA-A2. J Virol 80:8351–8361. https://doi.org/10.1128/JVI.00896-06.
54. Sidney J, Southwood S, Moore C, Oseroff C, Pinilla C, Grey HM, Sette A. 2013. Measurement of MHC/peptide interactions by gel filtration or monoclonal antibody capture. Curr Protoc Immunol Chapter 18:Unit 18.3. https://doi.org/10.1002/0471142735.im1803s100.
55. Harndahl M, Rasmussen M, Roder G, Dalgaard Pedersen I, Sorensen M, Nielsen M, Buus S. 2012. Peptide-MHC class I stability is a better predictor than peptide affinity of CTL immunogenicity. Eur J Immunol 42:1405–1416. https://doi.org/10.1002/eji.201141774.
56. St Leger AJ, Peters B, Sidney J, Sette A, Hendricks RL. 2011. Defining the herpes simplex virus-specific CD8+ T cell repertoire in C57BL/6 mice. J Immunol 186:3927–3933. https://doi.org/10.4049/jimmunol.1003735.
57. Gilchuk P, Spencer CT, Conant SB, Hill T, Gray JJ, Niu X, Zheng M, Erickson JJ, Boyd KL, McAfee KJ, Oseroff C, Hadrup SR, Bennink JR, Hildebrand W, Edwards KM, Crowe JE, Jr, Williams JV, Buus S, Sette A, Schumacher TN, Link AJ, Joyce S. 2013. Discovering naturally processed antigenic determinants that confer protective T cell immunity. J Clin Invest 123:1976–1987. https://doi.org/10.1172/JCI67388.
58. BenMohamed L, Wechsler SL, Nesburn AB. 2002. Lipopeptide vaccines—yesterday, today, and tomorrow. Lancet Infect Dis 2:425–431. https://doi.org/10.1016/S1473-3099(02)00318-3.
59. Nesburn AB, Bettahi I, Dasgupta G, Chentoufi AA, Zhang X, You S, Morishige N, Wahlert AJ, Brown DJ, Jester JV, Wechsler SL, BenMohamed L. 2007. Functional Foxp3+ CD4+ CD25Bright+ "natural" regulatory T cells are abundant in rabbit conjunctiva and suppress virus-specific CD4+ and CD8+ effector T cells during ocular herpes infection. J Virol 81:7647–7661. https://doi.org/10.1128/JVI.00294-07.
60. Mott KR, Chentoufi AA, Carpenter D, BenMohamed L, Wechsler SL, Ghiasi H. 2009. The role of a glycoprotein K (gK) CD8+ T-cell epitope of herpes simplex virus on virus replication and pathogenicity. Invest Ophthalmol Vis Sci 50:2903–2912. https://doi.org/10.1167/iovs.08-2957.
61. Beura LK, Hamilton SE, Bi K, Schenkel JM, Odumade OA, Casey KA, Thompson EA, Fraser KA, Rosato PC, Filali-Mouhim A, Sekaly RP, Jenkins MK, Vezys V, Haining WN, Jameson SC, Masopust D. 2016. Normalizing the environment recapitulates adult human immune traits in laboratory mice. Nature 532:512–516. https://doi.org/10.1038/nature17655.
62. Jing L, Laing KJ, Dong L, Russell RM, Barlow RS, Haas JG, Ramchandani MS, Johnston C, Buus S, Redwood AJ, White KD, Mallal SA, Phillips EJ, Posavad CM, Wald A, Koelle DM. 2016. Extensive CD4 and CD8 T cell cross-reactivity between alphaherpesviruses. J Immunol 196:2205–2218. https://doi.org/10.4049/jimmunol.1502366.
63. Cornberg M, Clute SC, Watkin LB, Saccoccio FM, Kim SK, Naumov YN, Brehm MA, Aslan N, Welsh RM, Selin LK. 2010. CD8 T cell cross-reactivity networks mediate heterologous immunity in human EBV and murine vaccinia virus infections. J Immunol 184:2825–2838. https://doi.org/10.4049/jimmunol.0902168.
64. Selin LK, Brehm MA, Naumov YN, Cornberg M, Kim SK, Clute SC, Welsh RM. 2006. Memory of mice and men: CD8+ T-cell cross-reactivity and heterologous immunity. Immunol Rev 211:164–181. https://doi.org/10.1111/j.0105-2896.2006.00394.x.
65. Selin LK, Welsh RM. 2004. Plasticity of T cell memory responses to viruses. Immunity 20:5–16. https://doi.org/10.1016/S1074-7613(03)00356-X.
66. Khan AA, Srivastava R, Spencer D, Garg S, Fremgen D, Vahed H, Lopes PP, Pham TT, Hewett C, Kuang J, Ong N, Huang L, Scarfone VM, Nesburn AB, Wechsler SL, BenMohamed L. 2015. Phenotypic and functional characterization of herpes simplex virus glycoprotein B epitope-specific effector and memory CD8+ T cells from symptomatic and asymptomatic individuals with ocular herpes. J Virol 89:3776–3792. https://doi.org/10.1128/JVI.03419-14.
67. Joshi NS, Cui W, Dominguez CX, Chen JH, Hand TW, Kaech SM. 2011. Increased numbers of preexisting memory CD8 T cells and decreased T-bet expression can restrain terminal differentiation of secondary effector and memory CD8 T cells. J Immunol 187:4068–4076. https://doi.org/10.4049/jimmunol.1002145.
68. Khan AA, Srivastava R, Lopes PP, Wang C, Pham TT, Cochrane J, Thai NT, Gutierrez L, BenMohamed L. 2014. Asymptomatic memory CD8 T cells: from development and regulation to consideration for human vaccines and immunotherapeutics. Hum Vaccin Immunother 10:945–963. https://doi.org/10.4161/hv.27762.
69. Hufner K, Horn A, Derfuss T, Glon C, Sinicina I, Arbusow V, Strupp M, Brandt T, Theil D. 2009. Fewer latent herpes simplex virus type 1 and cytotoxic T cells occur in the ophthalmic division than in the maxillary and mandibular divisions of the human trigeminal ganglion and nerve. J Virol 83:3696–3703. https://doi.org/10.1128/JVI.02464-08.
70. Miller JD, van der Most RG, Akondy RS, Glidewell JT, Albott S, Masopust D, Murali-Krishna K, Mahar PL, Edupuganti S, Lalor S, Germon S, Del Rio C, Mulligan MJ, Staprans SI, Altman JD, Feinberg MB, Ahmed R. 2008. Human effector and memory CD8+ T cell responses to smallpox and yellow fever vaccines. Immunity 28:710–722. https://doi.org/10.1016/j.immuni.2008.02.020.
71. Schwendemann J, Choi C, Schirrmacher V, Beckhove P. 2005. Dynamic differentiation of activated human peripheral blood CD8+ and CD4+ effector memory T cells. J Immunol 175:1433–1439. https://doi.org/10.4049/jimmunol.175.3.1433.
72. Chentoufi AA, Kritzer E, Tran MV, Dasgupta G, Lim CH, Yu DC, Afifi RE, Jiang X, Carpenter D, Osorio N, Hsiang C, Nesburn AB, Wechsler SL, BenMohamed L. 2011. The herpes simplex virus 1 latency-associated transcript promotes functional exhaustion of virus-specific CD8+ T cells in latently infected trigeminal ganglia: a novel immune evasion mechanism. J Virol 85:9127–9138. https://doi.org/10.1128/JVI.00587-11.
73. Chentoufi AA, Dervillez X, Dasgupta G, Nguyen C, Kabbara KW, Jiang X, Nesburn AB, Wechsler SL, BenMohamed L. 2012. The herpes simplex virus type 1 latency-associated transcript inhibits phenotypic and functional maturation of dendritic cells. Viral Immunol 25:204–215. https://doi.org/10.1089/vim.2011.0091.
74. Blackburn SD, Shin H, Haining WN, Zou T, Workman CJ, Polley A, Betts MR, Freeman GJ, Vignali DA, Wherry EJ. 2009. Coregulation of CD8+ T cell exhaustion by multiple inhibitory receptors during chronic viral infection. Nat Immunol 10:29–37. https://doi.org/10.1038/ni.1679.
75. Wherry EJ, Ha SJ, Kaech SM, Haining WN, Sarkar S, Kalia V, Subramaniam S, Blattman JN, Barber DL, Ahmed R. 2007. Molecular signature of CD8+ T cell exhaustion during chronic viral infection. Immunity 27:670–684. https://doi.org/10.1016/j.immuni.2007.09.006.
76. Barber DL, Wherry EJ, Masopust D, Zhu B, Allison JP, Sharpe AH, Freeman GJ, Ahmed R. 2006. Restoring function in exhausted CD8 T cells during chronic viral infection. Nature 439:682–687. https://doi.org/10.1038/nature04444.
77. Conrady CD, Zheng M, Stone DU, Carr DJ. 2012. CD8+ T cells suppress viral replication in the cornea but contribute to VEGF-C-induced lymphatic vessel genesis. J Immunol 189:425–432. https://doi.org/10.4049/jimmunol.1200063.
78. Verjans GM, Dings ME, McLauchlan J, van Der Kooi A, Hoogerhout P, Brugghe HF, Timmermans HA, Baarsma GS, Osterhaus AD. 2000. Intraocular T cells of patients with herpes simplex virus (HSV)-induced acute retinal necrosis recognize HSV tegument proteins VP11/12 and VP13/14. J Infect Dis 182:923–927. https://doi.org/10.1086/315759.
79. Oh S, Terabe M, Pendleton CD, Bhattacharyya A, Bera TK, Epel M, Reiter Y, Phillips J, Linehan WM, Kasten-Sportes C, Pastan I, Berzofsky JA. 2004. Human CTLs to wild-type and enhanced epitopes of a novel prostate and breast tumor-associated protein, TARP, lyse human breast cancer cells. Cancer Res 64:2610–2618. https://doi.org/10.1158/0008-5472.CAN-03-2183.
80. Stuber G, Leder GH, Storkus WT, Lotze MT, Modrow S, Szekely L, Wolf H, Klein E, Karre K, Klein G. 1994. Identification of wild-type and mutant p53 peptides binding to HLA-A2 assessed by a peptide loading-deficient cell line assay and a novel major histocompatibility complex class I peptide binding assay. Eur J Immunol 24:765–768. https://doi.org/10.1002/eji.1830240341.
81. Rubio V, Stuge TB, Singh N, Betts MR, Weber JS, Roederer M, Lee PP. 2003. Ex vivo identification, isolation and analysis of tumor-cytolytic T cells. Nat Med 9:1377–1382. https://doi.org/10.1038/nm942.
82. BenMohamed L, Krishnan R, Auge C, Primus JF, Diamond DJ. 2002. Intranasal administration of a synthetic lipopeptide without adjuvant induces systemic immune responses. Immunology 106:113–121. https://doi.org/10.1046/j.1365-2567.2002.01396.x.
83. Zhang X, Chentoufi AA, Dasgupta G, Nesburn AB, Wu M, Zhu X, Carpenter D, Wechsler SL, You S, BenMohamed L. 2009. A genital tract peptide epitope vaccine targeting TLR-2 efficiently induces local and systemic CD8+ T cells and protects against herpes simplex virus type 2 challenge. Mucosal Immunol 2:129–143. https://doi.org/10.1038/mi.2008.81.